Title

Multi-level Modulation of Light Signaling by GIGANTEA Regulates Both the Output and Pace of the Circadian Clock.

Journal

Developmental cell, 49(6)

ISSN

1534-5807

Authors

Nohales, Maria A
Liu, Wanlu
Duffy, Tomas
et al.

Publication Date

2019-06-01

DOI

10.1016/j.devcel.2019.04.030

Peer reviewed

HHS Public Access

Author manuscript

Dev Cell. Author manuscript; available in PMC 2020 June 17.

Published in final edited form as:

Dev Cell. 2019 June 17; 49(6): 840–851.e8. doi:10.1016/j.devcel.2019.04.030.

Multilevel modulation of light signaling by GIGANTEA regulates both the output and pace of the circadian clock

Maria A. Nohales[1], **Wanlu Liu**[2,3], **Tomas Duffy**[1], **Kazunari Nozue**[4], **Mariko Sawa**[5], **Jose L. Pruneda-Paz**[5], **Julin N. Maloof**[4], **Steven E. Jacobsen**[2,6], and **Steve A. Kay**[1,7,*]

[1]Keck School of Medicine, University of Southern California, Los Angeles, CA 90089, USA

[2]Department of Molecular, Cell, and Developmental Biology, University of California, Los Angeles, Los Angeles, CA 90095, USA

[3]Zhejiang University-University of Edinburgh Institute, Zhejiang University School of Medicine, 310058 Hangzhou, P. R. China

[4]Department of Plant Biology, University of California, Davis, Davis, CA 95616, USA

[5]Section of Cell and Developmental Biology, Division of Biological Sciences, University of California, San Diego, La Jolla, CA 92093, USA

[6]Howard Hughes Medical Institute, University of California, Los Angeles, Los Angeles, CA 90095, USA

[7]Lead Contact

SUMMARY

Integration of environmental signals with endogenous biological processes is essential for organisms to thrive in their natural environment. Being entrained by periodic environmental changes, the circadian clock incorporates external information to coordinate physiological processes, phasing them to the optimal time of the day and year. Here we present a pivotal role for the clock component GIGANTEA (GI) as a genome-wide regulator of transcriptional networks mediating growth and adaptive processes in plants. We provide mechanistic details on how GI integrates endogenous timing with light signaling pathways through the global modulation of PHYTOCHROME-INTERACTING FACTORs (PIFs). Gating of the activity of these transcriptional regulators by GI directly affects a wide array of output rhythms, including photoperiodic growth. Furthermore, we uncover a role for PIFs in mediating light input to the circadian oscillator and show how their regulation by GI is required to set the pace of the clock in response to light-dark cycles.

*Correspondence: stevekay@usc.edu.

AUTHOR CONTRIBUTIONS

Conceptualization, M.A.N. and S.A.K.; Investigation, M.A.N., W.L., T.D., M.S., J.L.P., and K.N.; Resources, J.N.M., S.E.J., and S.A.K.; Writing, M.A.N. and S.A.K.

DECLARATION OF INTERESTS

The authors declare no competing interests.

eTOC blurb

Nohales et al. show how the clock component GIGANTEA modulates light signaling pathways by gating the activity of PIFs at multiple regulatory levels. This function of GI is essential not only to optimize growth strategies in plants, but also to set the pace of the clock in response to light-dark cycles.

INTRODUCTION

Accurate decoding of environmental signals and integration of these cues within cellular networks is essential for organisms to succeed in their natural environment. The rhythmic and periodic nature of relevant external conditions, such as light and temperature oscillations, has driven the evolution of endogenous molecular oscillators that enable organisms to anticipate these cyclic changes and coordinate key physiological processes accordingly (Millar, 2016). In plants, adequate integration of environmental cues and precise phasing of biological processes are key, as their sessile growth habit precludes their escape from disadvantageous conditions. The influence of the circadian clock on plant development is pervasive. Multiple processes, including growth, stress responses, and developmental transitions, are coordinated by the clock in conjunction with other signaling pathways (Greenham and McClung, 2015; Sanchez and Kay, 2016). Clock genes and their feedback regulatory mechanisms have been extensively studied in plants (Nohales and Kay, 2016). However, little is known about how environmental information is transmitted to this complex network nor do we have mechanistic knowledge on how the clock regulates such a wide array of biological processes.

A key clock protein that seems to function at the interface between the oscillator and its output is GI, a conserved plant-specific protein expressed in the evening (Fowler et al., 1999; Park et al., 1999). GI is essential for accurate timekeeping and clock synchronization with the environment (Gould et al., 2006; Kim et al., 2007; Locke et al., 2006; Martin-Tryon et al., 2007; Mizoguchi et al., 2005). Besides its role in the central oscillator, GI modulates myriad clock output pathways, including abiotic stress (Cao et al., 2005; Kim et al., 2013a), photoperiodic flowering (Sawa et al., 2007; Suarez-Lopez et al., 2001), and light signaling (Huq et al., 2000; Martin-Tryon et al., 2007; Oliverio et al., 2007). Despite its pivotal role in clock function and plant development, knowledge of the mechanisms by which GI is able to influence such a wide array of cellular networks is only starting to emerge. At a post-translational level, GI interacts with multiple proteins from diverse pathways (Mishra and Panigrahi, 2015) and, recently, a role for GI as a co-chaperone (holdase) has been uncovered (Cha et al., 2017). In the context of transcriptional regulation, GI has been shown to influence transcription of flowering time genes through interaction with and modulation of their transcriptional regulators, as well as by occupancy of a small cluster of promoter regions (Sawa and Kay, 2011; Sawa et al., 2007).

Light signaling entails the perception of light quality and quantity by an array of photoreceptors specialized in sensing specific wavelengths of the light spectrum (Moglich et al., 2010), which then relay this information to transcriptional networks to ultimately regulate the expression of genes involved in light responses. In terms of light quality, the red

and far-red regions are especially relevant, and are perceived by the phytochrome (phy) family of photoreceptors (Xu et al., 2015). One of the mechanisms through which phytochromes achieve regulation of gene expression is through interaction with PIFs, a family of bHLH transcription factors that function as negative regulators of photomorphogenesis in the dark (Leivar and Monte, 2014; Xu et al., 2015). Notably, these factors carry out a broader function and act as hubs that integrate information from multiple cellular pathways, including light, temperature, hormone, and circadian signaling (Castillon et al., 2007; Legris et al., 2017; Leivar and Quail, 2011).

Previous studies have uncovered extensive connections between the oscillator and PIFs, and several clock components have been identified to regulate *PIF* expression and/or activity (Martin et al., 2018; Nieto et al., 2015; Soy et al., 2016; Zhu et al., 2016). Here we have investigated GI function in the context of transcriptional regulation and have uncovered direct connections of unprecedented complexity between this core clock component and PIFs. We show how GI globally modulates light signaling by gating the activity of the PIF proteins at multiple regulatory levels and, at the physiological level, we provide evidence regarding how this regulation influences output rhythms such as photoperiodic growth. Since PIF proteins function as hubs in the regulation of plant growth and development (Daviere and Achard, 2016; Leivar and Quail, 2011; Xu et al., 2014), broad modulation of their activity by GI provides a mechanism by which the circadian clock acts as an overarching hub for integrating environmental and endogenous signaling pathways to optimize adaptive traits in plants. Moreover, we uncover a critical role for the PIF proteins in light input to the circadian system and show that their regulation by GI is required for optimal clock progression, providing a molecular framework for understanding how light signaling entrains the plant circadian clock.

RESULTS

GI shares targets with both clock and light signaling pathways

We initiated our study of the molecular mechanisms of GI function in the context of transcriptional regulation by performing a reanalysis of published genome-wide gene expression datasets. A search for over-represented *cis* elements at the promoter regions of differentially expressed genes (DEGs) in the *gi-2* null mutant (Kim et al., 2012) revealed the G-box [CACGTG] and the evening element (EE) [(A)AAATATCT] as the two most highly enriched motifs (Figure 1A). The G-box motif is found in the promoters of many light regulated genes and is known to be bound by different transcription factors including the PIFs (Hornitschek et al., 2009; Huq and Quail, 2002; Martinez-Garcia et al., 2000), whereas the EE is bound by the morning core clock repressors CIRCADIAN CLOCK ASSOCIATED 1 (CCA1) and LATE ELONGATED HYPOCOTYL (LHY) (Alabadi et al., 2001) and is enriched at the promoters of genes with peak expression in the evening (Covington et al., 2008; Harmer et al., 2000).

Given the involvement of GI in light signaling and photomorphogenesis (Huq et al., 2000; Martin-Tryon et al., 2007) as well as in *CCA* and *LHY* expression (Fowler et al., 1999; Mizoguchi et al., 2002; Park et al., 1999), we decided to subsequently analyze the overlap between DEGs in *gi-2* (Kim et al., 2012) and a comprehensive set of PIF-regulated genes

(Oh et al., 2012) or DEGs in *cca1–1;lhy-11* (Kamioka et al., 2016). In spite of the diversity of conditions under which these legacy datasets were obtained, this analysis rendered two subsets of significantly shared genes with distinct characteristics (Figures 1B and S1A). The subset of genes shared by GI and PIFs is most highly enriched in Gene Ontology (GO) terms related to photosynthesis, light signaling, and response to abiotic stress, and is enriched in peak expression phases around dawn (Zeitgeber time 23 (ZT23) to ZT1) and morning/early afternoon (ZT2 to ZT5), especially under short day (SD) conditions (Figures 1C and S1B,D). In contrast, genes shared by GI and CCA1 and LHY are involved in pathways related to circadian rhythms, temperature acclimation, response to diverse abiotic stimuli, and response to gibberellins (Figure S1D). In this case, analysis of time-of-day expression further revealed that these genes tend to be expressed in the evening, mostly at ZT11 to ZT14 (Figure S1C).

These results support the notion that GI plays dual roles in the regulation of light signaling and the circadian system, consistent with earlier genetic analyses (Martin-Tryon et al., 2007; Mizoguchi et al., 2005; Oliverio et al., 2007). Genes shared by GI and CCA1/LHY are clock components and clock outputs whose evening-phased expression is likely driven by the EE, supporting a key role for GI in the central oscillator and in the regulation of *CCA* and *LHY* amplitude (Fowler et al., 1999; Mizoguchi et al., 2002; Park et al., 1999). Conversely, GI and PIFs seem to intersect at a subset of genes for the regulation of photosynthesis, light signaling, and growth promotion at the end of the night.

GI interacts with PIFs

GI acts as a positive regulator of light signal transduction and photomorphogenesis (Huq et al., 2000; MartinTryon et al., 2007), and *gi* mutant plants display a long hypocotyl phenotype under different light conditions (Figure S1E). While GI affects the expression of several clock factors, which in turn interact with and regulate the function of PIFs (Martin et al., 2018; Nieto et al., 2015; Soy et al., 2016; Zhu et al., 2016), we wondered if GI function in the light signaling pathway could also arise from a direct connection to PIFs. Given the ability of GI to interact and modulate the activity of diverse proteins, we hypothesized that interaction with PIF proteins may provide a molecular framework for understanding the mechanism by which GI directly regulates light signaling transcriptional networks. Leveraging an arrayed *Arabidopsis* transcription factor library (Pruneda-Paz et al., 2014), we performed a high-throughput yeast two-hybrid screen using GI as bait. We found that GI is able to strongly interact with PIF3, and to a lesser extent with other PIFs such as PIF1, PIF4 and PIF5, in this system (Figure S1F,G).

Through *in vitro* pull-down assays using full-length and deleted protein fragments, we verified the observed interactions (Figure 1D), and mapped the interaction domains for PIF3 (Figure S1H). These deletion studies showed that GI likely interacts with the bHLH DNA-binding motif of PIF3, suggesting that the interaction could hinder PIF3 binding to chromatin. We further confirmed the interaction of GI with PIF3 and PIF5 *in vivo* by performing co-immunoprecipitation (co-IP) studies in transgenic *Arabidopsis thaliana* seedlings expressing tagged protein versions (Figure 1E).

GI modulates PIF stability and activity

Given the physical interaction between GI and PIFs through a region containing the bHLH domain, we hypothesized that GI could function to prevent the access of PIFs to their target promoters and/or affect their stability. In fact, gene expression analyses of PIF target genes revealed that these are significantly altered in *gi-2* and GIox plants across the entire day and even more significantly during the night period (Figures 2A and S2A). Although GI affects *PIF4* and *PIF5* mRNA expression during the early night (de Montaigu et al., 2015; Fornara et al., 2015) (Figure S2B), this observation seems insufficient to explain the dramatic effect observed on PIF target gene expression.

Transient stability analyses revealed a modest effect of GI on HA-PIF3 protein accumulation (Figure S2C), which was not evident for HA-PIF5 (Figure S2D). More significantly, we observed that GI co-expression promoted a shift in the migration pattern of both PIFs suggestive of post-translational modification. A treatment with phosphatase was observed to reverse the mobility shift (Figure S2E), indicating that it is dependent upon phosphorylation. Because PIF phosphorylation is linked to their degradation (Ni et al., 2013; Shen et al., 2008), the results globally suggested that GI may affect PIF accumulation *in vivo*. Subsequent analysis of PIF5 protein accumulation at ZT8 and 16 in the Arabidopsis lines expressing tagged versions of GI and PIF5 confirmed that PIF5-HA accumulation is strongly affected by GI overexpression *in vivo* (Figures 2B and S2F).

We next performed transient transcriptional activation assays and measured activation of the *pPIL1*::LUC reporter (promoter of the well-characterized PIF target gene *PHYTOCHROME INTERACTING FACTOR 3-LIKE 1* (*PIL1)* driving the expression of the luciferase gene) as a proxy for PIF activity in the presence and absence of GI. In these experiments, PIF overexpression resulted in activation of the reporter as expected (Figures 2C and S2G), except in the case of PIF3, for which activation could not be assessed under our experimental conditions. In all cases, co-expression of GI together with the PIF effectors led to a drastic reduction in *pPIL1* promoter activation (Figures 2C and S2G). Given that GI affects PIF protein levels, we next examined whether the observed effect of GI on PIF transcriptional activity may also arise from a sequestration mechanism, similarly to the DELLA proteins (de Lucas et al., 2008; Feng et al., 2008; Li et al., 2016). To test this hypothesis, we performed *in vitro* electrophoretic mobility shift assays (EMSAs) with proteins expressed in an *in vitro* transcription and translation system (Martinez-Garcia et al., 2000). In these experiments, the binding of Flag-PIF3 to a *PIL1* promoter fragment containing two G-boxes was reduced in the presence of HA-GI (Figure S2H), even though Flag-PIF3 levels remained unchanged and GI does not bind the DNA probe directly (Figure S2I,J). A similar result was also obtained for Flag-PIF5 (Figure S2K). Altogether, consistent results across this set of *in planta*, *in vivo*, and *in vitro* experiments strongly suggest that GI interaction with PIF proteins directly interferes with their stability as well as with their DNA binding activity *in vivo*.

In order to characterize the effect of GI on PIF association to genomic targets *in vivo*, we performed chromatin immunoprecipitation (ChIP) assays. To uncouple transcriptional regulation of *PIF* expression by GI, we took advantage of the HA-PIF5 overexpression lines (Lorrain et al., 2008), both in Col-0 and a GIox (GI-YPET-Flag) background. To further

uncouple the effect of GI on PIF stability, we also leveraged the PIF3-ECFP-HA overexpression line, because a detailed characterization of this line indicated that the ECFP tag might increase PIF3 stability (Janczak et al., 2015) without affecting its primary functions such as DNA binding and phyB mediated degradation. Specifically, we observed that the accumulation of the PIF3-ECFP-HA fusion protein showed no significant differences when GI is overexpressed both in tobacco and in Arabidopsis (Figure S3A–C). Furthermore, a treatment with PAC, previously shown to affect PIF3 stability (Li et al., 2016), was also ineffective in promoting the degradation of PIF3-ECFP-HA as opposed to PIF5-HA (Figure S3D,E), further suggesting that the ECFP tag may be stabilizing it. Despite this increased stability, the fusion protein is still sensitive to degradation through major regulatory mechanisms such as phyB-mediated degradation, and when expressed under the control of its endogenous promoter it accumulates during the night period as expected (Soy et al., 2012) (Figure S3G). Importantly, it also proved to be functional because plants overexpressing it display longer hypocotyls under different light conditions (Kim et al., 2003) and show up-regulation of PIF target genes such as *PIL1* (Figure S3F). Using these lines in our ChIP experiments, for both PIF5 and PIF3 we observed a significantly reduced enrichment of the G-box containing regions in the promoter of *PIL1* in the immunoprecipitated fractions in the presence of GI at all ZTs tested (Figures 2D and S3H) with a subsequent reduction in *PIL1* mRNA expression (Figure 2E). Conversely, mutation of *GI* resulted in a greater enrichment of the same genomic regions when PIF3 was immunoprecipitated (Figures 2F and S3I), and this greater binding resulted in higher *PIL1* expression at night (Figure 2G). Because in the PIF3-ECFP-HA lines PIF3 protein levels are not affected by GI (Figure S3A–G), our results suggest that GI affects PIF binding to target chromatin not only indirectly by affecting their stability, but also directly by preventing their binding to specific sites within the chromatin.

If differential stability and activity of PIF proteins underlies the increased expression levels of PIF target genes observed in *gi-2* mutant plants, loss of *PIFs* is expected to reverse this phenotype. As predicted by our hypothesis, loss of *PIF3*, *PIF4*, and *PIF5* drastically reduced the expression of *PIL1* and *LONG HYPOCOTYL IN FAR-RED 1* (*HFR1*) in *gi-2* seedlings grown under SD conditions (Figures 2H and S3J,K), and this molecular phenotype also results in a reduction of hypocotyl elongation (Figure 2I). Notably, we observed that genes repressed by PIFs such as *PHYTOENE SYNTHASE* (*PSY*) are downregulated in *gi-2*, and this downregulation was also rescued by loss of *PIF3*, *PIF4*, and *PIF5* (Figure S3L). These observations suggest that GI-mediated modulation of PIF activity might be relevant for the regulation of multiple PIF regulated processes, including growth and chlorophyll and carotenoid biosynthesis.

GI and PIFs occupy the same targets genome-wide in a phase dependent pattern

Even though GI does not seem to bind DNA directly (Figure S2J), previous reports from our laboratory and others have shown that it is able to associate with chromatin (Kim et al., 2013b; Sawa and Kay, 2011; Sawa et al., 2007). We therefore decided to further investigate this association and to test whether GI may additionally prevent PIF binding to chromatin by occupying common target sites *in vivo*. To this end, we analyzed GI occupancy at the promoter regions bound by PIFs in *Arabidopsis* transgenic lines expressing tagged GI driven

by an endogenous promoter fragment. We observed that GI occupies PIF target regions at dusk and more significantly during the early night (ZT8 and 10), but not later in the night (ZT16) (Figure 3A). This trend correlates well with the observed GI accumulation pattern: under SD conditions, *GI* mRNA peaks at around ZT8, with GI protein levels being highest during the early night and then progressively declining (David et al., 2006; Kim et al., 2007; Sawa et al., 2007) (Figure S4A). On the other hand, PIF accumulation increases as the night period progresses (Figure S4A) and, consistently, PIF3 binding to target sites increases following the same trend (Soy et al., 2016) (Figure 3B). This phased protein accumulation and chromatin occupancy pattern of GI and PIFs, together with the effect of GI mis-regulation on PIF target gene expression, suggests a function of GI in restricting PIF activity during the early night in order to prevent rapid PIF-mediated regulation of gene expression immediately after transitioning to darkness. In support of this hypothesis, interaction between GI and PIFs was observed to increase as the night progresses peaking at ZT15–16 (Figure S4B,C), and we observe a more significant effect of GI on PIF binding to target genes at night (Figure 2D–G, S3H,I), as well as a higher and more rapid induction of PIF target genes upon darkness in the absence of GI compared to wildtype plants (Figure 3C).

To further test our model, we performed genome-wide analyses of GI genomic targets by ChIP followed by deep sequencing (ChIP-seq). These studies revealed that GI preferentially associates to promoter and intergenic regions (hypergeometric test p-value=8.6e–644 and 6.1e–109, respectively) (Figures 3D and S4D,E) and its targets include over 35% of genes found to be misregulated in *gi-2* seedlings in a previous study (Kim et al., 2012) (Figure 3E), which is indicative of a function of GI in the regulation of gene expression. Importantly, motif overrepresentation analysis of GI binding sites revealed the G-box as the most highly enriched *cis* element (Figure 3F). Comparison of GI and PIF3 ChIP-seq experiments under SD conditions (performed at ZT8 and ZT16, respectively) revealed that GI binds a significant set of PIF3 targets (p-value<0.01) (Figures 3G and S4F,G) which are enriched in GO terms related to multiple pathways known to be regulated by PIFs (Leivar and Monte, 2014; Leivar and Quail, 2011) (Figure S4H). Moreover, genes shared by GI and PIF3 tend to be expressed at the end of the night and during the morning/early afternoon in SDs, consistent with genes that are induced and repressed by PIFs (Figure S4I). These results suggest a function of GI as a regulator of PIF transcriptional targets genome-wide. Further comparison of GI and PIF3 binding peaks revealed that both proteins co-localize and bind to the same sites genome-wide (Figures 3H,I and S4J), strengthening the hypothesis that they GI binding may affect PIF access to genomic regions. To gain further insight into how GI regulates PIF3 chromatin accessibility, we performed PIF3 quantitative ChIP-seq experiments with internal spike-in standards in the wildtype and *gi-2* backgrounds. As expected, we observed an overall increment of PIF3 binding to chromatin in the absence of *GI* (Figure 3J). Furthermore, genomic regions with the highest GI binding signal (top 10%) showed a statistically significant greater increment of PIF3 binding in the absence of *GI*, than genomic regions with moderate or weak GI binding (Figures 3K and S4K). Altogether, our results suggest that GI globally affects PIF3 association to chromatin and more specifically regulates a subset of PIF3 target genes by binding to them and hindering PIF access to regulatory regions. This provides an additional timing mechanism to delay PIF

activity and adequately phase the expression of PIF targets to the most appropriate time of the day.

The physiological relevance of our findings for output rhythmicity is evidenced by GI function in the regulation of photoperiodic growth, for example, where GI is required to appropriately phase growth rhythms towards the end of the night under SD photoperiods. Growth rhythm measurements in SDs showed that *gi-2* mutant plants display a general growth de-repression, which is especially notable during the early night (Figure S4L), as previously reported (Nozue et al., 2007). Loss of *PIF3*, however, partially rescued not only the average growth rate phenotype, but also shifted the maximal growth phase to peak later (Figure S4L).

GI modulation of light signaling affects circadian rhythms

The molecular and physiological interactions between GI and PIFs revealed by our studies provide compelling evidence for how the circadian clock and light signaling pathways intersect for the regulation of output pathways. The observation that PIF3 and GI share targets related to circadian rhythms (Figure S4H) and the fact that both proteins bind to the promoter of the core clock gene *CCA1* around the same region *in vivo* (Figure 4A) prompted us to further investigate the relevance of the GI-PIF interaction for the regulation of circadian rhythmicity. Gene expression analyses implied that PIFs repress the expression of *CCA1* under SD conditions (see expression levels in *pifQ* as compared to wildtype plants, Figure 4B). This observation was further confirmed by transient activation assays using the *pCCA1*::LUC reporter, which showed that PIFs are able to repress *pCCA1* activity (Figure S5A). Notably, mutation of *PIFs* alleviated the very low level of *CCA1* expression in *gi-2* mutants (Figures 4B,C and S5B), suggesting that excessive PIF activity in *gi-2* may (at least partially) be responsible for the low amplitude of *CCA1* in this mutant. At the level of *pCCA1* promoter activation, it also proved to be de-repressed in *pif4–101;pif5–1* mutants, more significantly during the dark to light transitions (Figure S5C). Consistent with the gene expression analyses, loss-of-function mutation of *PIF3*, *PIF4*, and *PIF5* significantly rescued the low amplitude phenotype of *pCCA1* oscillations in *gi-2*, especially in anticipation of the light phase and at dusk (Figure 4D).

Analysis of *pCCA1* promoter activity in *Arabidopsis* seedlings under free running conditions revealed that, although consistent with previous reports *pif3–1* mutation does not show an obvious period phenotype (Viczian et al., 2005), *pif4–101;pif5–1* double mutants display a lengthened period in our experimental conditions (Figure S5D,E). Conversely, PIF overexpression lines displayed shorter periods than wildtype plants (Figure S5F,G), confirming the role of PIF proteins in determining the pace of the clock under these conditions. More importantly, loss of *PIF3* in the *gi-2* background increased the amplitude of *pCCA1* oscillations and lengthened the short period of *gi-2* mutants by 1 hour (Figures 4E,F and S5H,I). The double *gi-2;pif3–1* mutants also maintained *pCCA1* rhythmicity for longer under free running conditions compared to *gi-2* seedlings, which displayed less robust oscillations with higher relative amplitude error (RAE) and became arrhythmic after the third day in constant light (Figure 4E). On the other hand, loss of both *PIF4* and *PIF5* also lengthened the period of *gi-2* mutant seedlings by 1 hour, but in this case the oscillations in

the triple *gi-2;pif4–101;pif5–1* mutants were less robust and seedlings lost rhythmicity very soon under free running conditions (Figures 4G,H and S5J,K). These results not only suggest that *PIF* mis-regulation contributes to the circadian phenotype observed in *gi-2* mutants, but also that PIF3 and PIF4/PIF5 play partially non overlapping roles in this process. We subsequently analyzed the role of PIFs in light-responsive expression of *CCA1* by monitoring *pCCA1* activity in 3 day old etiolated seedlings transferred to light. In these experiments, we observed a significantly higher increase in the light-induced *pCCA1* activation in *pif4–101;pif5–1* compared to wildtype plants (Figure 4I). On the contrary, this activation was strongly repressed in PIF overexpression lines (Figure S5L). And in line with our previous results, PIF mutation significantly increased *pCCA1* light-responsiveness in *gi-2* (Figure 4I). Finally, the role of PIFs in the light input pathway to the oscillator was further investigated by analyzing *pCCA1*::LUC phase resetting in response to light pulses at specific ZTs. These experiments revealed that, while the *pif3–1* mutation does not have a significant effect consistent with previous reports (Viczian et al., 2005), *pif4–101;pif5–1* double mutants display a more pronounced phase delay in response to light, especially during the early night (Figure S5M).

Taken together, our results uncover a role of PIF proteins in light input to the circadian system, directly linking light signaling to *CCA1* transcriptional regulation. We also show that modulation of PIF activity by GI is not only required to adequately phase output rhythms such as growth, but also for proper clock progression and light input.

DISCUSSION

Precise timing of physiological processes by the circadian clock provides an adaptive advantage for most organisms (Millar, 2016). In plants, many developmental processes, including photoperiodic growth, are tightly coordinated by the circadian clock, which integrates a variety of internal and external signals (Greenham and McClung, 2015; Sanchez and Kay, 2016). The molecular features required for the efficient decoding and integration of the multiple stimuli perceived within these complex regulatory networks are only just becoming apparent. Here we provide evidence for a mechanism directly linking a component of the circadian oscillator to the gating of light signaling pathways (Figure 5). Our evidence supports a model where GI directly regulates the activity of the master regulators of light signaling in plants, the PIF proteins, thereby gating the sensitivity to external signals to ultimately shape plant development across the light-dark cycle.

GI modulates light signaling by globally interfering with PIF activity. Importantly, our data indicate that GI affects PIF activity at multiple levels, including *PIF* transcription, PIF degradation, and PIF access to target chromatin. Our observation that GI promotes PIF phosphorylation is especially intriguing, because phosphorylation of PIF proteins, which leads to their subsequent ubiquitination and degradation, is a key module of the signal transduction pathway by which photo-activated photoreceptors trigger the expression of light-responsive genes (Ni et al., 2013; Xu et al., 2015). GI interacts with phyB in yeast and *in planta* (Yeom et al., 2014), but it is unknown whether this interaction occurs *in vivo* and what its functional implications may be. In parallel, a recent study has shown that Photoregulatory Protein Kinases (PPKs) catalyze the photoactivated-phy-induced

phosphorylation of PIF3 (Ni et al., 2017). These kinases interact with the Evening Complex through phyB and are involved in circadian rhythmicity and hypocotyl elongation (Zheng et al., 2018); more recently, their function in the latter has been shown to involve synergistic and antagonistic interactions with CCA1 and RGA, respectively (Zheng et al., 2018). It is tempting to speculate that GI may enhance interaction of PIFs with phyB and/or specific protein kinases, such as PPKs. Detailed studies will be required to unravel how GI mediates phosphorylation of PIFs, if it is involved in the aforementioned pathways, what other co-factors are required, and its functional relevance in the context of light signal transduction.

The finding that GI affects PIF binding to target promoters not only through direct binding but also by occupying common target regions is a remarkable one and provides evidence of a mechanism that differentiates GI from the other core clock components, such as EARLY FLOWERING 3 (ELF3) and the PRRs (PSEUDO-RESPONSE REGULATORS), which interact with PIFs and repress their activity at growth-promoting genes without affecting their stability and/or their association to target regions (Martin et al., 2018; Nieto et al., 2015; Soy et al., 2016; Zhu et al., 2016). Notably, our genome-wide studies extend GI function as a general regulator of PIFs well beyond the control of hypocotyl elongation, affecting a wide array of pathways in which these transcriptional hubs are involved. To what extent and how GI regulates these other transcriptional networks, what timing properties are delivered by it, and what its impact is on overall plant fitness will be important questions to be addressed in future studies.

The biochemical function of GI, a key component of the circadian oscillator in plants, has long been elusive, partially due to the lack of well characterized functional domains within the protein and such a broad array of mutant allele phenotypes. The notion of GI as a scaffold protein is widely accepted, given its ability to interact with a multiplicity of partners (Mishra and Panigrahi, 2015). More recently, a function as a holdase that enhances HSP90/HSP70-mediated maturation of the blue-light photoreceptor ZEITLUPE (ZTL) (Cha et al., 2017) has been proposed. Our work takes an important step towards understanding more broadly the molecular function of GI and how it is able to exert its regulatory functions across a wide swath of physiology. We find that GI binds the promoter regions of thousands of genes involved in diverse biological processes. And even though experiments were performed under different conditions, over a third of genes found to be misregulated in *gi-2* in a previous study are indeed bound by GI, suggesting direct regulation of GI target genes at the transcriptional level. Given that GI does not appear to associate to the DNA directly, an important question will be to uncover the mechanisms by which it is recruited to the chromatin. The finding of the G-box as the most highly enriched motif around GI ChIP-seq peaks points to a G-box binding transcription factor (or different ones) involved in this recruitment. A plausible candidate would be ELONGATED HYPOCOTYL 5 (HY5). HY5 plays an antagonistic role to PIFs and binds a common set of target promoters in a phased pattern (Toledo-Ortiz et al., 2014), similarly to GI. Nevertheless, it is very likely that other DNA binding transcription factors are also involved, because other motifs were also overrepresented around GI peaks and GI targets an ample set of genes that are not bound by PIFs. Whether GI is targeted through the recognition of specific chromatin features such as specific histone marks is also unknown. The identification of the factors that recruit GI to the

chromatin, as well as those that are recruited by GI, will be necessary to fully understand the role of GI in the regulation of transcription.

Finally, our study provides evidence on the involvement of PIFs in the light input pathway to the oscillator and how GI modulation of PIF activity is required not only to regulate output processes, but also to maintain proper clock progression. Earlier work suggested a role for PIF proteins in the circadian clock (Martinez-Garcia et al., 2000), but this implication could not be subsequently confirmed using PIF3 single mutants and overexpression lines (Viczian et al., 2005) likely due to the high level of redundancy among PIFs. More recently, ChIP-seq experiments have revealed the binding of PIFs to the promoters of clock genes *in vivo* (Oh et al., 2012; Zhang et al., 2013), and the interaction between PIFs and several clock components has been reported (Martin et al., 2018; Nieto et al., 2015; Soy et al., 2016; Zhu et al., 2016). Additionally, a recent study has shown the implication of PIFs in metabolic signaling to the clock (Shor et al., 2017). Our results show that PIFs can directly repress *CCA1* during the night, most remarkably at the light to dark transitions, and PIF function is required for period length determination. Successive mutation of *PIFs* in *gi-2* progressively increased *CCA1* amplitude in this mutant and alleviated its short period phenotype, which suggests that excessive PIF activity is at least partially responsible for the canonical clock phenotype of *gi-2* mutants. Nevertheless, mutation of PIF genes only partially rescued *gi-2* circadian phenotypes, implicating that additional mechanisms take place in the regulation of *CCA1* expression by GI and in GI function in the circadian system. Different PIFs also seemed to affect *gi-2* rhythmicity differently, which suggests that they may have both overlapping and distinct roles in the system. This could provide mechanisms for differential transcriptional regulation of, or physical interaction with, other clock components. It is also remarkable that the effect of *PIF4* and *PIF5* mutation on *CCA1* phase resetting in response to light is more pronounced in the middle of the night. The specific function of the different PIFs in the circadian system, their dynamics in time, and their interaction with other input pathways will need to be unraveled to fully understand how clock phase is set in response to light.

Altogether, our study assigns a role to GI as a pivotal integrator of external and internal signals to regulate both the circadian clock and its output in the context of transcriptional regulation, and provides a mechanistic framework to further investigate the circadian gating of plant development and how light signals are transmitted into the circadian system.

STAR METHODS

CONTACT FOR REAGENT AND RESOURCE SHARING

Further information and requests for resources and reagents should be directed to and will be fulfilled by the Lead Contact, Steve A. Kay (stevekay@usc.edu).

EXPERIMENTAL MODEL AND SUBJECT DETAILS

Plant material and growth conditions—Wildtype, mutant, and transgenic lines used in this study were *Arabidopsis thaliana* ecotype Columbia 0 (Col-0). *gi-2* (Fowler et al., 1999), GIox (David et al., 2006), PIF5-HA (Lorrain et al., 2008), PIF4-Flash (Pedmale et al., 2016),

pif3–1 (SALK_030753) (Kim et al., 2003), *pif4–101* (Garlic_114_G06) (Lorrain et al., 2008), *pif5–1* (SALK_087012) (Fujimori et al., 2004), *pifQ* (Leivar et al., 2008), and CCA1::LUC (Salome and McClung, 2005) have been previously described. *pif3–1* and *pifQ* lines were obtained from the Arabidopsis Biological Research Center (ABRC) collection. The *gi-2* mutation is a deletion (Δ670–677) that introduces a premature stop codon and is considered a null mutation predicted to encode a nonfunctional 114 aa polypeptide rather than the 1173 aa GI protein (Fowler et al., 1999).

Seeds were chlorine gas sterilized and plated on 0.5x Linsmaier and Skoog medium (LS, Caisson Laboratories) with 0.8% agar (Sigma). After stratification in the dark at 4 °C for 3 days, plates were transferred to a Percival incubator (Percival-scientific.com) set to the indicated light conditions with light supplied at 80% mol m^{-2} s^{-1} by cool-white fluorescent bulbs and a constant temperature of 22 °C.

Generation of plant lines—*gi-2;pif3–1*, *gi-2;pif4–101*, *gi-2;pif5–1* and *gi-2;pif4–101;pif5–1* higher order mutants were generated by genetic crosses between single and double mutants, and homozygous mutant lines were identified in the F2 populations by PCR amplification with primers listed in supplemental Table S2.

PIF3-ECFP-HA;GI-YPET-Flag and PIF3-ECFP-HA;*gi-2* lines were obtained by crossing a transgenic line overexpressing PIF3-ECFP-HA (hygromycin resistance) with a transgenic line overexpressing GI-YPET-Flag (BASTA resistant and *gi-2*). F3 populations were scored for hygromycin resistance and BASTA resistance/sensitivity. The presence of the *gi-2* allele in both lines was determined by PCR amplification with primers listed in supplemental Table S2. PIF5-HA was crossed with GI-YPET-Flag to obtain PIF5-HA;GI-YPET-Flag. F3 populations were scored for seed coat GFP fluorescence and BASTA resistance. The presence of the *gi-2* allele was determined by PCR amplification with primers listed in supplemental Table S2. For co-immunoprecipitation studies, F2 segregating populations derived from these crosses were used.

The transgenic PIF3-ECFP-HA and GI-YPET-Flag lines were generated by Agrobacterium-mediated floral dip transformation of Col-0 and *gi-2* plants, respectively. To this purpose, *Agrobacterium tumefaciens* strain GV3101 was transformed with the binary vectors pH-35S::PIF3-ECFP-HA, pH-pPIF3::PIF3-ECFP-HA, pB-35S::GI-YPET-Flag, and pB-pGI::GI-YPET-Flag (described below), respectively. Functionality of the fusion proteins was determined phenotypically. PIF3-ECFP-HA overexpressing plants displayed longer hypocotyls under both SD and continuous light and were hyposensitive to red light. On the contrary, GI-YPET-Flag overexpressing plants displayed shorter hypocotyls under both SD and continuous light. The GI-YPET-Flag transgene also rescued the late flowering phenotype of *gi-2* plants.

To obtain the different reporter lines expressing *pCCA1*::LUC, the mutant lines *gi-2;pif3–1*, *gi-2;pif4-101;pif5-1*,and the PIF overexpressing lines PIF3-ECFP-HA, PIF5-HA, and PIF4-Flash were crossed with the CCA1::LUC line (BASTA resistance). *pCCA1*::LUC homozygous lines were identified in the F3 population by scoring BASTA resistance and the

presence of the different mutant alleles and transgenes was determined by PCR amplification with primers listed in supplemental Table S2.

METHOD DETAILS

Construction of binary vectors—The binary vectors used for co-localization studies in *Nicotiana benthamiana* and the generation of transgenic *Arabidopsis* lines were constructed by MultiSite Gateway Three-Fragment Vector Technology (Invitrogen). Full-length cDNAs encoding PIF3 (without the stop codon) were amplified by PCR and cloned into the pENTR/D-TOPO vector (Invitrogen) (primers used are listed in supplemental Table S2). pENTR-GI-stop (Sawa and Kay, 2011) and pENTR-PIF5 (Pruneda-Paz et al., 2014) have been described earlier. pENTR-PIF5 was mutagenized by PCR using the primers listed in supplemental Table S2 to eliminate the stop codon. In the case of the endogenous *PIF3* and *GI* promoter sequences, 2000 bp upstream of the *PIF3* start codon or 2533 bp upstream of the *GI* start codon (Berns et al., 2014) were amplified by PCR using the primers listed in supplemental Table S2 and cloned into the pDONR P4–P1R vector (Invitrogen) by Gateway BP recombination reaction (Invitrogen). The pDONR P4–P1R vector containing the 35S promoter sequence was a gift from Joanne Chory (The SALK Institute, La Jolla, CA). The sequences of YPET and ECFP-HA (from pEarleyGate102 (Earley et al., 2006)) were subcloned into the pDONR P2R-P3 vector (primer listed in supplemental Table S2). pDONR P2R-P3-YPET was subsequently modified by PCR-based mutagenesis to introduce a Flag tag (primers used are listed in supplemental Table S2). Selected promoter, gene, and fluorescent tag combinations were finally cloned by MultiSite Gateway reaction (Invitrogen) into either pH7m34GW (35S::PIF3-ECFP-HA and pPIF3::PIF3-ECFP-HA) or pB7m34GW (35S::GI-YPET-Flag and pB-pGI::GI-YPET-Flag) binary destination vectors from the University of Ghent collection (https://gateway.psb.ugent.be).

To perform protein stability and transactivation assays in transient expression in *N. benthamiana*, the cDNAS encoding GI, PIF1, PIF3, PIF4, PIF5, and GFP were amplified by PCR from the pENTR/D-TOPO vector (primers used are listed in supplemental Table S2) and subcloned into the pDONR207 vector (Invitrogen) by Gateway BP recombination reaction (Invitrogen). Subsequently, they were transferred to either pEarleyGate201 or pEarleyGate202 (Earley et al., 2006) (pEG) binary destination vectors by Gateway LR recombination reaction (Invitrogen). The sequences introduced into these plasmids contained stop codon. Specifically, the different constructs generated and used were as follow: pEG201-GFP, pEG202-GI, pH-35S::PIF3-ECFP-HA, pEG201-PIF3, and pEG201-PIF5 were used for protein stability analyses, and pEG202-PIF1, pEG202-PIF3, pEG202-PIF4, pEG202-PIF5, pEG201-GI, and pEG201-GFP were used for transient transcriptional activation assays. To prepare the reporter constructs for the transactivation assays, the promoter sequences of *PIL1* (2066 bp upstream of the start codon) and *CCA1* (1140 bp upstream of the start codon) were amplified by PCR from genomic DNA (primers used are listed in supplemental Table S2) and cloned into the XhoI and BamHI sites of the pGreenII 0800-LUC vector (Hellens et al., 2005).

Yeast two-hybrid analyses—The ProQuest™ Two-Hybrid System (Invitrogen) was used to perform yeast two-hybrid (Y2H) analyses. The cDNA encoding full-length GI was

transferred from the pENTR/D-TOPO vector (Invitrogen) into the pDEST32 vector by Gateway LR recombination reaction (Invitrogen) to generate the bait plasmid. The pDEST22 prey plasmids containing the sequences encoding PIF1, PIF3, PIF4, and PIF5 have been previously described (Pruneda-Paz et al., 2014). Empty pDEST22 and the pExpAD502 plasmids were used as negative controls. All Y2H procedures were performed following the manufacturer's instructions. Quantitation of β-galactosidase activity was performed in a 96-well format as previously described (Pruneda-Paz et al., 2009).

***In vitro* pull-downs—**For *in vitro* pull-down assays, additional constructs were made. The pENTR/D-TOPO plasmids (Invitrogen) containing the sequences encoding GI, PIF1, and PIF5 have been previously described (Pruneda-Paz et al., 2014; Sawa and Kay, 2011). Full-length *PIF3*, *PIF4*, and *GFP* sequences were amplified by PCR (primers used are listed in supplemental Table S2) and cloned into the pENTR/D-TOPO vector (Invitrogen). Partial *PIF3* sequences were amplified by PCR (primers used are listed in supplemental Table S2) and cloned into the pDONRZeo vector (Invitrogen) by Gateway BP recombination reaction (Invitrogen). To express proteins in the cell-free system, all inserts were transferred by Gateway LR recombination reaction (Invitrogen) into Gateway compatible modified pTnT vectors (Promega) (Nito et al., 2013), which were kindly provided by Dr. Joanne Chory (The SALK Institute, La Jolla, CA). The vectors contained an N-terminal HA or Flag tag as specified in each case. Proteins were co-expressed using TnT® SP6 High-Yield Wheat Germ Protein Expression System (Promega) as per manufacturer's instructions. Five percent of the reactions (2.5 μl) were used to verify expression of the proteins (input) and the remaining extract was immunoprecipitated as earlier described (Pedmale et al., 2016) using anti-HA 3F10 antibody (Roche).

Transient expression in *N. benthamiana*—*Agrobacterium tumefaciens* strain GV3101 was used in all instances, except for the constructs derived from the pGreenII 0800-LUC vector, which were transformed into the *A. tumefaciens* strain C58 containing the pSoup helper plasmid. *A. tumefaciens* cells containing the respective constructs and the p19 silencing suppressor were grown overnight at 28 °C in liquid LB medium supplemented with the appropriate antibiotics. Cultures were pelleted, resuspended in 10 mM MES-KOH pH 5.6, 10 mM $MgCl_2$, 150 μM acetosyringone to a final OD_{600} of 0.5, and incubated for 2h at room temperature. The suspensions were then mixed and infiltrated in *N. benthamiana* leaves at a final OD_{600}=0.1 each, except for p19 which was infiltrated at a final OD_{600}=0.05. Samples were harvested 2 days post-inoculation (dpi) for transactivation assays and 3 dpi for co-localization and protein stability analyses. In the case of MG-132 treatments, plants were infiltrated with 25 μM MG-132 8h before harvesting.

Protein immunoprecipitation—Approximately 1 g of 10-day-old *Arabidopsis* seedlings grown in SDs were harvested at ZT 8 and frozen in liquid nitrogen. For time-course experiments, 0.5 g were used. Immunoprecipitations were performed as earlier described (Nusinow et al., 2011) with the following modifications. Samples were ground with mortar and pestle in liquid nitrogen and resuspended in 2 ml of modified SII buffer (100 mM NaPhosphate, pH 8.0, 150 mM NaCl, 5 mM EDTA, 5 mM EGTA, 0.1% Triton X-100, 2 mM PMSF, 1x protease inhibitor cocktail (Roche), 1x Phosphatase Inhibitors 2&3 (Sigma)

and 50 μM MG-132 (Peptides International)). Extracts were transferred to a dounce tissue grinder and homogenized before being clarified twice by centrifugation at 4 °C. Total protein concentration was quantified by DC Protein Assay (Bio-Rad), and normalized to 1.875 mg/ml. Three percent of the extracts was used to verify proteins levels (input). For immunoprecipitation, extracts were incubated with anti-Flag M2 antibody (Sigma) for 2 h with gentle rotation at 4 °C. Subsequently, 25 μl of magnetic protein G Dynabeads (Invitrogen) pre-washed with IP buffer were added to the samples and incubated for 2 h with gentle rotation at 4 °C. The samples were finally washed 3x with modified SII buffer and the precipitated protein was eluted by heating beads at 95 °C for 5 min in 40μl of 2x SDS-PAGE loading buffer. 10 and 30 μl of the eluate were separately analyzed by Western blot to detect the immunoprecipitated and co-immunoprecipitated proteins, respectively.

Protein stability and accumulation analyses—To determine protein levels in transient experiments in *N. benthamiana*, samples were homogenized with 3 volumes of 2x SDS-PAGE loading buffer and boiled at 95 °C for 5 min. Samples were then clarified by centrifugation at room temperature and analyzed by Western blot. For normalization, GFP-HA or p19-HA were used as internal loading controls. Alkaline phosphatase treatments were performed as earlier described (Ni et al., 2013) with the following modifications. Proteins were extracted with 2x SDS-PAGE loading buffer, boiled at 95 °C for 5 min, and clarified by centrifugation. Extracted proteins were diluted 10-fold into reaction buffer (50 mM Tris-HCl pH 8.8, 100 mM NaCl, 50 mM $MgCl_2$, 1% Triton X-100, 1x protease inhibitor cocktail (Roche)) and incubated in the presence or absence of CIP (400 U/ml) for 2h at 37 °C. Samples were then analyzed by Western blot.

For the analysis of PIF3-ECFP-HA and PIF5-HA protein levels in *Arabidopsis* seedlings, samples were homogenized with 100 μl of extraction buffer (50 mM Tris-HCl pH 7.6, 150 mM NaCl, 5 mM $MgCl_2$, 0.1% NP-40, 10% glycerol, 2 mM PMSF, 1x protease inhibitor cocktail (Roche), 1x Phosphatase Inhibitors 2&3 (Sigma) and 50 μM MG-132 (Peptides International)) and clarified twice by centrifugation at 4 °C. Total protein concentration was quantified by DC Protein Assay (Bio-Rad) and 40 ug of each sample was subsequently analyzed by Western blot. ACTIN levels in the samples were used for normalization.

Western blot detection and quantitation—Protein extracts in SDS-PAGE loading buffer were boiled at 95 °C for 5 min and separated in 4–15 % SDS-PAGE gels. Proteins were then transferred to nitrocellulose membranes (BioRad), which were then stained with Ponceau S to assess transfer and loading. Finally, membranes were immunodetected with either Horse Radish Peroxidase (HRP)-conjugated 3F10 anti-HA (1:2000, Roche) or HRP-conjugated Flag M2 (1:2000, Sigma) antibody. The ACTIN loading control was detected using anti-ACTIN C4 mouse antibody (1:500, Millipore) followed by HRP-conjugated anti-mouse secondary antibody (1:3000, BioRad). *Arabidopsis* PIF3-ECFP-HA and PIF5-HA blots were cut at the 50 kDa mark and the upper and lower parts were detected with anti-HA and anti-ACTIN antibodies, respectively. Chemiluminescence was detected with the Supersignal West Pico, Dura, and Femto substrates (Pierce) and imaged with a UVP ChemiDoc imaging system (UVP, LLC) (in which case the VisionWorksLS (UVP, LLC) software was used to quantify protein levels) or captured by exposure of X-ray films (GE

Healthcare), which were scanned and protein levels quantified using NIH ImageJ software (Schneider et al., 2012) (https://imagej.nih.gov/ij/).

Electrophoretic mobility shift assay (EMSA)—DNA probes for gel-shift assays (Martinez-Garcia et al., 2000) were generated by annealing the oligonucleotides listed in supplemental Table S2 (N629+N630 for the labeled probe, and N602+N603 for the unlabeled one). Proteins were produced by *in vitro* transcription and translation (Martinez-Garcia et al., 2000) using the TnT® SP6 High-Yield Wheat Germ Protein Expression System (Promega) as per manufacturer's instructions. Binding reactions were prepared by mixing the indicated amounts of protein solutions in binding buffer (10 mM Tris-HCl pH 7.5, 50 mM KCl, 1 mM DTT, 5 mM $MgCl_2$, 2.5% glycerol, 0.05% NP-40) containing 1 μg poly (dI-dC) and 1 μl of the end-labeled probe (100 nM) in a final volume of 20 μl. For competitions, the indicated amounts of unlabeled probe or protein extract were added to the reaction. After incubation for 20 minutes at room temperature, complexes were resolved by 6% PAGE in 0.5x TBE buffer at room temperature. Gels were scanned with a Typhoon 9410 imager (GE Healthcare).

RNA extraction and qRT-PCR—Total RNA was isolated with the GeneJET plant RNA purification mini kit (Thermo Scientific). For cDNA synthesis, 1μg of total RNA was digested with DNase I (Roche) and reverse-transcribed using the iScript cDNA synthesis kit (Bio-Rad). Synthesized cDNA was amplified by real-time quantitative PCR (qPCR) with Maxima SYBR Green qPCR Master Mix (Thermo Scientific) using the CFX-384 Real Time System (BioRad).*PROTEIN PHOSPHATASE 2A* (*PP2A*) (AT1G13320) was used as the normalization control. Primer sequences are listed in supplemental Table S2.

Transactivation assays—Reporter and effector constructs were co-infiltrated in *N. benthamiana* leaves and 2 dpi transient activation assays were performed as earlier described (Nieto et al., 2015).

Chromatin immunoprecipitation (ChIP)—Approximately 4 g of fresh weight whole seedlings were harvested at the indicated ZTs and cross-linked with 1% formaldehyde under vacuum for 10 min. Cross-linking was quenched by adding glycine to a final concentration of 125 mM, pH 8.0 under vacuum for 5 min. Seedlings were then washed three times in ddH20 and rapidly frozen in liquid nitrogen. Samples were ground with mortar and pestle in liquid nitrogen and processed as described (Sawa et al., 2007) with the following modifications: lysed nuclei were diluted 4-fold with ChIP dilution buffer (16.7 mM Tris-HCl pH 8, 167 mM NaCl, 1.1% Triton X-100, 1.2 mM EDTA, 1nM PMSF, 5mM Benzamadine, 1x protease inhibitor cocktail (Roche)) and sonicated using a Bioruptor (Diagenode) (0.5 s on/off cycles for 15 min total at maximum power) to shear DNA to an average size of 500–1000 bp. After sonication, samples were clarified twice by centrifugation at 4 °C and the chromatin solution was diluted 2-fold with ChIP dilution buffer and pre-cleared by adding 50 μl of magnetic protein G Dynabeads (Invitrogen) pre-washed with ChIP dilution buffer for 1 h with gentle rotation at 4 °C. At this point, 100 μl were saved as input. Immunoprecipitation was then performed overnight with 4 ug of anti-HA 3F10 (Roche) or anti-Flag M2 (Sigma) antibody at 4 °C with gentle rotation. Mock samples were processed

without antibody. Subsequently, 50 µl of magnetic protein G Dynabeads (Invitrogen) pre-washed with ChIP dilution buffer were added and samples were incubated for 2 h with gentle rotation at 4 °C. Low and high salt washes were followed by LiCl buffer (250 mM LiCl, 1% Sodium Deoxycholate, 1% NP-40, 1 mM EDTA) and TE buffer (10 mM Tris-HCl pH 8, 1 mM EDTA) washes. Immunocomplexes were eluted twice from the beads using a modified elution buffer (100 mM $NaHCO_3$, 10 mM EDTA, 1% SDS) and incubation at 65 °C. Crosslinking in the immunoprecipitated and input samples was reversed by adding NaCl to a final concentration of 200 mM and incubating at 65°C overnight, which was followed by a treatment with Proteinase K (Invitrogen) to degrade all proteins. DNA was purified by phenol-chloroform extraction and ethanol precipitation. DNA was resuspended in 75 µl of TE and 1 l aliquots were used for qPCR. For the input samples, 1 µl of a 100-fold dilution was used for qPCR. qPCR reactions were performed in triplicate with Maxima SYBR Green qPCR Master Mix (Thermo Scientific) using the Stratagene Mx3005P qPCR system (Agilent Technologies). Primers used were as in previous studies (Johnson et al., 2014; Nieto et al., 2015; Soy et al., 2016) and are listed in supplemental Table S2. Enrichment in each sample was calculated relative to the input and expressed in percentage.

ChIP-seq—ChIP-seq libraries were prepared with the NuGEN Ovation® Ultralow System as per manufacturer's instructions. For quantitative ChIP-seq, 0.02 ng of sonicated unmethylated lambda DNA (Promega) were added to each sample prior to library preparation.

Physiological measurements—To analyze hypocotyl length, evenly spaced seedlings were grown on plates under the indicated light conditions and photoperiod. At the specified time, seedlings were scanned and images were analyzed using NIH ImageJ software (https://imagej.nih.gov/ij/).

For growth rate analyses, plants were grown and analyzed essentially as described (Nozue et al., 2007) except that the growth media was 1/2X MSMO (Sigma), 0.8% phytagar (Sigma) and images were captured with a PixeLINK PL-A781 camera driven by LabView (National Instruments). Plants were grown under short day cycles (8h light, 16 h dark) at 22 °C in a Conviron E7 plant growth chamber. 72 µmol m^{-2} s^{-1} photosynthetically active radiation was provided by cool white fluorescent bulbs.

Clock activity measurements—For circadian rhythm measurements, seedlings were grown on 96-well plates and entrained in SD conditions. After 7 days of entrainment, 500 µM luciferin (Biosynth AG) was added to the wells and the plates were transferred to constant light (80 µmol m^{-2} s^{-1}). Bioluminescence was recorded for 5 days. Diel monitoring of *pCCA1*::LUC expression was conducted similarly, except that seedlings were kept in SDs while recording over the course of 2 days. In order to analyze the light-induced activation of *pCCA1*, etiolated seedlings were grown on 96-well plates for 3 days in constant darkness after stratification and germination induction. Bioluminescence started to be recorded immediately after transfer to constant white light. Light-induced phase shifts of *pCCA1*::LUC expression were quantified as earlier described (Viczian et al., 2005). Briefly, seedlings were grown under SDs for 5 days, and then kept in continuous darkness for 24 h. After 24 h in darkness, plates were irradiated with white light at the indicated ZTs for 1 h

and then transferred to the luminometer to monitor luminescence. Phase shifts were calculated by comparing the phase values of the pulsed plants with those of non-pulsed controls. In all cases, bioluminescence was recorded every 1 h over the indicated period of time with a Tecan Infinite M200 plate reader (with the exception of Figure 4E and S2G - PIF1 and PIF4 panels, for which a Centro LB960 Microplate Luminometer (Berthold Technologies) was used due to logistic reasons) and data were analyzed by fast Fourier transformed non-linear least squares (FFT-NLLS) using BioDare2 (Moore et al., 2014; Zielinski et al., 2014) (https://www.biodare2.ed.ac.uk). For phase shift calculations, the LS Periodogram algorithm was applied (Zielinski et al., 2014).

QUANTIFICATION AND STATISTICAL ANALYSIS

Mean comparisons—In order to test the statistical significance of the difference between mean values relative to wildtype controls, Student's *t*-test and Tukey's multiple comparisons test were applied, as specified in each experiment. Sample size and number of replicates (where applicable) for each experiment are indicated in the respective figure legend. Information about types of tissue can be found in the respective figure legend and in the Method Details section. Strategies for randomization and/or stratification and sample size estimation were not applied to these experiments. No statistical calculation was used to estimate the sample size.

ChIP-seq data analysis—Raw sequencing reads from the sequencer were demultiplexed and quality controlled with FastQC (v0.11.3). Reads with high quality were then aligned to the Arabidopsis reference genome (TAIR10) with Bowtie (v1.0.0) (Langmead et al., 2009), allowing only uniquely mapping reads with fewer than two mismatches, and duplicated reads were combined into one read. For quantitative ChIP-seq, reads were also mapped to lambda DNA with Bowtie (v1.0.0) (Langmead et al., 2009) with the same parameters as before. For both Flag and HA ChIP-seqs, peaks were called with MACS2 (v 2.1.1.) (Zhang et al., 2008) using Flag and HA ChIP-seqs in Col-0 as controls, respectively. The set of peaks identified from both the GI and PIF3 ChIP-seqs can be found in the supplemental Table S1 file. In all cases, ChIP-seq signal was measured in reads per kilobase million (RPKM), and normalized to the signal in the control Col-0 IP. For quantitative ChIP-seq, the signal was additionally normalized to the lambda DNA spike-in control. ChIP-seq metaplots were plotted using NGSplot (v 2.41.4) (Shen et al., 2014). *De novo* predominant motifs analysis was conducted using HOMER (Heinz et al., 2010) over a 200 bp region around the ChIP-seq peak summits.

Genome-wide gene expression analyses—All datasets used for genome-wide gene expression analysis are compiled in the supplemental Table S1.

The statistical significance of the overlap between gene lists was calculated using Fisher's exact test.

Identification of over-represented known plant transcription factor binding motifs at 1000 bp promoter regions of DEGs in *gi-2* seedlings (Kim et al., 2012) was performed with HOMER (Heinz et al., 2010).

The web-based tool Phaser (http://phaser.mocklerlab.org/) (Mockler et al., 2007) was used to determine the phases of peak gene expression and their over-representation.

For the identification of over-represented Gene Ontology (GO) categories in gene lists, the web-based tool PANTHER (http://www.pantherdb.org/) (Thomas et al., 2003) was used. For the significantly enriched categories (p-value<0.05) in each subset, enrichment scores were calculated as $-\log_{10}(p)$, where p is the p-value from the enrichment analysis.

Growth rate calculations—Change in growth was calculated for each 30-min time interval and local polynomial regression fitting (loess) smoothing with smoothing parameter = 0.1 was used in R (RCoreTeam, 2016) and results were plotted with the ggplot2 plotting package (Wickham, 2009). Analysis scripts are available at https://github.com/MaloofLab/Nohales-2017.

DATA AND SOFTWARE AVAILABILITY

High-throughput sequencing data that support the findings in this study can be accessed through Gene Expression Omnibus (GEO) database with accession number GSEXXXXX.

Supplementary Material

Refer to Web version on PubMed Central for supplementary material.

ACKNOWLEDGEMENTS

We thank R. McClung and J. Chory for seeds and reagents, and N. Buceta, M. Akhter, and S. King for technical assistance. We also thank J. Gallego-Bartolome, S. Sanchez, D. Alabadi, and D. Nusinow for critical reading of the manuscript. This work was supported by the National Institute of General Medical Sciences of the National Institutes of Health under award numbers RO1GM067837 and RO1GM056006 to S.A.K. J.N.M. and K.N. acknowledge United States Department of Agriculture USDA NIFA project CA-D-PLB-7226-H and UC Davis for funding. S.E.J. is an investigator from the Howard Hughes Medical Institute.

REFERENCES

Alabadi D, Oyama T, Yanovsky MJ, Harmon FG, Mas P, and Kay SA (2001). Reciprocal regulation between TOC1 and LHY/CCA1 within the Arabidopsis circadian clock. Science 293, 880–883. [PubMed: 11486091]

Berns MC, Nordstrom K, Cremer F, Toth R, Hartke M, Simon S, Klasen JR, Burstel I, and Coupland G (2014). Evening expression of arabidopsis GIGANTEA is controlled by combinatorial interactions among evolutionarily conserved regulatory motifs. Plant Cell 26, 3999–4018. [PubMed: 25361953]

Cao S, Ye M, and Jiang S (2005). Involvement of GIGANTEA gene in the regulation of the cold stress response in Arabidopsis. Plant Cell Rep 24, 683–690. [PubMed: 16231185]

Castillon A, Shen H, and Huq E (2007). Phytochrome Interacting Factors: central players in phytochrome-mediated light signaling networks. Trends Plant Sci 12, 514–521. [PubMed: 17933576]

Cha JY, Kim J, Kim TS, Zeng Q, Wang L, Lee SY, Kim WY, and Somers DE (2017). GIGANTEA is a co-chaperone which facilitates maturation of ZEITLUPE in the Arabidopsis circadian clock. Nat Commun 8, 3. [PubMed: 28232745]

Covington MF, Maloof JN, Straume M, Kay SA, and Harmer SL (2008). Global transcriptome analysis reveals circadian regulation of key pathways in plant growth and development. Genome Biol 9, R130. [PubMed: 18710561]

David KM, Armbruster U, Tama N, and Putterill J (2006). Arabidopsis GIGANTEA protein is post-transcriptionally regulated by light and dark. FEBS Lett 580, 1193–1197. [PubMed: 16457821]

Daviere JM, and Achard P (2016). A Pivotal Role of DELLAs in Regulating Multiple Hormone Signals. Mol Plant 9, 10–20. [PubMed: 26415696]

de Lucas M, Daviere JM, Rodriguez-Falcon M, Pontin M, Iglesias-Pedraz JM, Lorrain S, Fankhauser C, Blazquez MA, Titarenko E, and Prat S (2008). A molecular framework for light and gibberellin control of cell elongation. Nature 451, 480–484. [PubMed: 18216857]

de Montaigu A, Giakountis A, Rubin M, Toth R, Cremer F, Sokolova V, Porri A, Reymond M, Weinig C, and Coupland G (2015). Natural diversity in daily rhythms of gene expression contributes to phenotypic variation. Proc Natl Acad Sci U S A 112, 905–910. [PubMed: 25548158]

Earley KW, Haag JR, Pontes O, Opper K, Juehne T, Song K, and Pikaard CS (2006). Gateway-compatible vectors for plant functional genomics and proteomics. Plant J 45, 616–629. [PubMed: 16441352]

Feng S, Martinez C, Gusmaroli G, Wang Y, Zhou J, Wang F, Chen L, Yu L, Iglesias-Pedraz JM, Kircher S, et al. (2008). Coordinated regulation of Arabidopsis thaliana development by light and gibberellins. Nature 451, 475–479. [PubMed: 18216856]

Fornara F, de Montaigu A, Sanchez-Villarreal A, Takahashi Y, Ver Loren van Themaat E, Huettel B, Davis SJ, and Coupland G (2015). The GI-CDF module of Arabidopsis affects freezing tolerance and growth as well as flowering. Plant J 81, 695–706. [PubMed: 25600594]

Fowler S, Lee K, Onouchi H, Samach A, Richardson K, Morris B, Coupland G, and Putterill J (1999). GIGANTEA: a circadian clock-controlled gene that regulates photoperiodic flowering in Arabidopsis and encodes a protein with several possible membrane-spanning domains. EMBO J 18, 4679–4688. [PubMed: 10469647]

Fujimori T, Yamashino T, Kato T, and Mizuno T (2004). Circadian-controlled basic/helix-loop-helix factor, PIL6, implicated in light-signal transduction in Arabidopsis thaliana. Plant Cell Physiol 45, 1078–1086. [PubMed: 15356333]

Gould PD, Locke JC, Larue C, Southern MM, Davis SJ, Hanano S, Moyle R, Milich R, Putterill J, Millar AJ, et al. (2006). The molecular basis of temperature compensation in the Arabidopsis circadian clock. Plant Cell 18, 1177–1187. [PubMed: 16617099]

Greenham K, and McClung CR (2015). Integrating circadian dynamics with physiological processes in plants. Nat Rev Genet 16, 598–610. [PubMed: 26370901]

Harmer SL, Hogenesch JB, Straume M, Chang HS, Han B, Zhu T, Wang X, Kreps JA, and Kay SA (2000). Orchestrated transcription of key pathways in Arabidopsis by the circadian clock. Science 290, 2110–2113. [PubMed: 11118138]

Heinz S, Benner C, Spann N, Bertolino E, Lin YC, Laslo P, Cheng JX, Murre C, Singh H, and Glass CK (2010). Simple combinations of lineage-determining transcription factors prime cis-regulatory elements required for macrophage and B cell identities. Mol Cell 38, 576–589. [PubMed: 20513432]

Hellens RP, Allan AC, Friel EN, Bolitho K, Grafton K, Templeton MD, Karunairetnam S, Gleave AP, and Laing WA (2005). Transient expression vectors for functional genomics, quantification of promoter activity and RNA silencing in plants. Plant Methods 1, 13. [PubMed: 16359558]

Hornitschek P, Lorrain S, Zoete V, Michielin O, and Fankhauser C (2009). Inhibition of the shade avoidance response by formation of non-DNA binding bHLH heterodimers. EMBO J 28, 3893–3902. [PubMed: 19851283]

Huq E, and Quail PH (2002). PIF4, a phytochrome-interacting bHLH factor, functions as a negative regulator of phytochrome B signaling in Arabidopsis. EMBO J 21, 2441–2450. [PubMed: 12006496]

Huq E, Tepperman JM, and Quail PH (2000). GIGANTEA is a nuclear protein involved in phytochrome signaling in Arabidopsis. Proc Natl Acad Sci U S A 97, 9789–9794. [PubMed: 10920210]

Janczak M, Bukowski M, Gorecki A, Dubin G, Dubin A, and Wladyka B (2015). A systematic investigation of the stability of green fluorescent protein fusion proteins. Acta biochimica Polonica 62, 407–411. [PubMed: 26192770]

Johnson LM, Du J, Hale CJ, Bischof S, Feng S, Chodavarapu RK, Zhong X, Marson G, Pellegrini M, Segal DJ, et al. (2014). SRA- and SET-domain-containing proteins link RNA polymerase V occupancy to DNA methylation. Nature 507, 124–128. [PubMed: 24463519]

Kamioka M, Takao S, Suzuki T, Taki K, Higashiyama T, Kinoshita T, and Nakamichi N (2016). Direct Repression of Evening Genes by CIRCADIAN CLOCK-ASSOCIATED1 in the Arabidopsis Circadian Clock. Plant Cell 28, 696–711. [PubMed: 26941090]

Kim J, Yi H, Choi G, Shin B, and Song PS (2003). Functional characterization of phytochrome interacting factor 3 in phytochrome-mediated light signal transduction. Plant Cell 15, 2399–2407. [PubMed: 14508006]

Kim WY, Ali Z, Park HJ, Park SJ, Cha JY, Perez-Hormaeche J, Quintero FJ, Shin G, Kim MR, Qiang Z, et al. (2013a). Release of SOS2 kinase from sequestration with GIGANTEA determines salt tolerance in Arabidopsis. Nat Commun 4, 1352. [PubMed: 23322040]

Kim WY, Fujiwara S, Suh SS, Kim J, Kim Y, Han L, David K, Putterill J, Nam HG, and Somers DE (2007). ZEITLUPE is a circadian photoreceptor stabilized by GIGANTEA in blue light. Nature 449, 356–360. [PubMed: 17704763]

Kim Y, Lim J, Yeom M, Kim H, Kim J, Wang L, Kim WY, Somers DE, and Nam HG (2013b). ELF4 regulates GIGANTEA chromatin access through subnuclear sequestration. Cell Rep 3, 671–677. [PubMed: 23523352]

Kim Y, Yeom M, Kim H, Lim J, Koo HJ, Hwang D, Somers D, and Nam HG (2012). GIGANTEA and EARLY FLOWERING 4 in Arabidopsis Exhibit Differential Phase-Specific Genetic Influences over a Diurnal Cycle. Mol Plant.

Langmead B, Trapnell C, Pop M, and Salzberg SL (2009). Ultrafast and memory-efficient alignment of short DNA sequences to the human genome. Genome Biol 10, R25. [PubMed: 19261174]

Legris M, Nieto C, Sellaro R, Prat S, and Casal JJ (2017). Perception and signalling of light and temperature cues in plants. Plant J 90, 683–697. [PubMed: 28008680]

Leivar P, and Monte E (2014). PIFs: systems integrators in plant development. Plant Cell 26, 56–78. [PubMed: 24481072]

Leivar P, Monte E, Oka Y, Liu T, Carle C, Castillon A, Huq E, and Quail PH (2008). Multiple phytochrome-interacting bHLH transcription factors repress premature seedling photomorphogenesis in darkness. Curr Biol 18, 1815–1823. [PubMed: 19062289]

Leivar P, and Quail PH (2011). PIFs: pivotal components in a cellular signaling hub. Trends Plant Sci 16, 19–28. [PubMed: 20833098]

Li K, Yu R, Fan LM, Wei N, Chen H, and Deng XW (2016). DELLA-mediated PIF degradation contributes to coordination of light and gibberellin signalling in Arabidopsis. Nat Commun 7, 11868. [PubMed: 27282989]

Locke JC, Kozma-Bognar L, Gould PD, Feher B, Kevei E, Nagy F, Turner MS, Hall A, and Millar AJ (2006). Experimental validation of a predicted feedback loop in the multi-oscillator clock of Arabidopsis thaliana. Mol Syst Biol 2, 59. [PubMed: 17102804]

Lorrain S, Allen T, Duek PD, Whitelam GC, and Fankhauser C (2008). Phytochrome-mediated inhibition of shade avoidance involves degradation of growth-promoting bHLH transcription factors. Plant J 53, 312–323. [PubMed: 18047474]

Martin-Tryon EL, Kreps JA, and Harmer SL (2007). GIGANTEA acts in blue light signaling and has biochemically separable roles in circadian clock and flowering time regulation. Plant Physiol 143, 473–486. [PubMed: 17098855]

Martin G, Rovira A, Veciana N, Soy J, Toledo-Ortiz G, Gommers CMM, Boix M, Henriques R, Minguet EG, Alabadi D, et al. (2018). Circadian Waves of Transcriptional Repression Shape PIF-Regulated Photoperiod-Responsive Growth in Arabidopsis. Curr Biol 28, 311–318 e315. [PubMed: 29337078]

Martinez-Garcia JF, Huq E, and Quail PH (2000). Direct targeting of light signals to a promoter element-bound transcription factor. Science 288, 859–863. [PubMed: 10797009]

Millar AJ (2016). The Intracellular Dynamics of Circadian Clocks Reach for the Light of Ecology and Evolution. Annu Rev Plant Biol 67, 595–618. [PubMed: 26653934]

Mishra P, and Panigrahi KC (2015). GIGANTEA - an emerging story. Front Plant Sci 6, 8. [PubMed: 25674098]

Mizoguchi T, Wheatley K, Hanzawa Y, Wright L, Mizoguchi M, Song HR, Carre IA, and Coupland G (2002). LHY and CCA1 are partially redundant genes required to maintain circadian rhythms in Arabidopsis. Developmental cell 2, 629–641. [PubMed: 12015970]

Mizoguchi T, Wright L, Fujiwara S, Cremer F, Lee K, Onouchi H, Mouradov A, Fowler S, Kamada H, Putterill J, et al. (2005). Distinct roles of GIGANTEA in promoting flowering and regulating circadian rhythms in Arabidopsis. Plant Cell 17, 2255–2270. [PubMed: 16006578]

Mockler TC, Michael TP, Priest HD, Shen R, Sullivan CM, Givan SA, McEntee C, Kay SA, and Chory J (2007). The DIURNAL project: DIURNAL and circadian expression profiling, model-based pattern matching, and promoter analysis. Cold Spring Harb Symp Quant Biol 72, 353–363. [PubMed: 18419293]

Moglich A, Yang X, Ayers RA, and Moffat K (2010). Structure and function of plant photoreceptors. Annu Rev Plant Biol 61, 21–47. [PubMed: 20192744]

Moore A, Zielinski T, and Millar AJ (2014). Online period estimation and determination of rhythmicity in circadian data, using the BioDare data infrastructure. Methods Mol Biol 1158, 13–44. [PubMed: 24792042]

Ni W, Xu SL, Chalkley RJ, Pham TN, Guan S, Maltby DA, Burlingame AL, Wang ZY, and Quail PH (2013). Multisite light-induced phosphorylation of the transcription factor PIF3 is necessary for both its rapid degradation and concomitant negative feedback modulation of photoreceptor phyB levels in Arabidopsis. Plant Cell 25, 2679–2698. [PubMed: 23903316]

Ni W, Xu SL, Gonzalez-Grandio E, Chalkley RJ, Huhmer AFR, Burlingame AL, Wang ZY, and Quail PH (2017). PPKs mediate direct signal transfer from phytochrome photoreceptors to transcription factor PIF3. Nat Commun 8, 15236. [PubMed: 28492231]

Nieto C, Lopez-Salmeron V, Daviere JM, and Prat S (2015). ELF3-PIF4 interaction regulates plant growth independently of the Evening Complex. Curr Biol 25, 187–193. [PubMed: 25557667]

Nito K, Wong CC, Yates JR 3rd, and Chory J (2013). Tyrosine phosphorylation regulates the activity of phytochrome photoreceptors. Cell Rep 3, 1970–1979. [PubMed: 23746445]

Nohales MA, and Kay SA (2016). Molecular mechanisms at the core of the plant circadian oscillator. Nat Struct Mol Biol 23, 1061–1069. [PubMed: 27922614]

Nozue K, Covington MF, Duek PD, Lorrain S, Fankhauser C, Harmer SL, and Maloof JN (2007). Rhythmic growth explained by coincidence between internal and external cues. Nature 448, 358–361. [PubMed: 17589502]

Nusinow DA, Helfer A, Hamilton EE, King JJ, Imaizumi T, Schultz TF, Farre EM, and Kay SA (2011). The ELF4-ELF3-LUX complex links the circadian clock to diurnal control of hypocotyl growth. Nature 475, 398–402. [PubMed: 21753751]

Oh E, Zhu JY, and Wang ZY (2012). Interaction between BZR1 and PIF4 integrates brassinosteroid and environmental responses. Nat Cell Biol 14, 802–809. [PubMed: 22820378]

Oliverio KA, Crepy M, Martin-Tryon EL, Milich R, Harmer SL, Putterill J, Yanovsky MJ, and Casal JJ (2007). GIGANTEA regulates phytochrome A-mediated photomorphogenesis independently of its role in the circadian clock. Plant Physiol 144, 495–502. [PubMed: 17384162]

Park DH, Somers DE, Kim YS, Choy YH, Lim HK, Soh MS, Kim HJ, Kay SA, and Nam HG (1999). Control of circadian rhythms and photoperiodic flowering by the Arabidopsis GIGANTEA gene. Science 285, 1579–1582. [PubMed: 10477524]

Pedmale UV, Huang SS, Zander M, Cole BJ, Hetzel J, Ljung K, Reis PA, Sridevi P, Nito K, Nery JR, et al. (2016). Cryptochromes Interact Directly with PIFs to Control Plant Growth in Limiting Blue Light. Cell 164, 233–245. [PubMed: 26724867]

Pruneda-Paz JL, Breton G, Nagel DH, Kang SE, Bonaldi K, Doherty CJ, Ravelo S, Galli M, Ecker JR, and Kay SA (2014). A genome-scale resource for the functional characterization of Arabidopsis transcription factors. Cell Rep 8, 622–632. [PubMed: 25043187]

Pruneda-Paz JL, Breton G, Para A, and Kay SA (2009). A functional genomics approach reveals CHE as a component of the Arabidopsis circadian clock. Science 323, 1481–1485. [PubMed: 19286557]

RCoreTeam (2016). R: A language and environment for statistical computing. R Foundation for Statistical Computing, Vienna, Austria URL https://www.R-project.org/.

Salome PA, and McClung CR (2005). PSEUDO-RESPONSE REGULATOR 7 and 9 are partially redundant genes essential for the temperature responsiveness of the Arabidopsis circadian clock. Plant Cell 17, 791–803. [PubMed: 15705949]

Sanchez SE, and Kay SA (2016). The Plant Circadian Clock: From a Simple Timekeeper to a Complex Developmental Manager. Cold Spring Harb Perspect Biol 8.

Sawa M, and Kay SA (2011). GIGANTEA directly activates Flowering Locus T in Arabidopsis thaliana. Proc Natl Acad Sci U S A 108, 11698–11703. [PubMed: 21709243]

Sawa M, Nusinow DA, Kay SA, and Imaizumi T (2007). FKF1 and GIGANTEA complex formation is required for day-length measurement in Arabidopsis. Science 318, 261–265. [PubMed: 17872410]

Schneider CA, Rasband WS, and Eliceiri KW (2012). NIH Image to ImageJ: 25 years of image analysis. Nat Methods 9, 671–675. [PubMed: 22930834]

Shen H, Zhu L, Castillon A, Majee M, Downie B, and Huq E (2008). Light-induced phosphorylation and degradation of the negative regulator PHYTOCHROME-INTERACTING FACTOR1 from Arabidopsis depend upon its direct physical interactions with photoactivated phytochromes. Plant Cell 20, 1586–1602. [PubMed: 18539749]

Shen L, Shao N, Liu X, and Nestler E (2014). ngs.plot: Quick mining and visualization of next-generation sequencing data by integrating genomic databases. BMC Genomics 15, 284. [PubMed: 24735413]

Shor E, Paik I, Kangisser S, Green R, and Huq E (2017). PHYTOCHROME INTERACTING FACTORS mediate metabolic control of the circadian system in Arabidopsis. New Phytol 215, 217–228. [PubMed: 28440582]

Soy J, Leivar P, Gonzalez-Schain N, Martin G, Diaz C, Sentandreu M, Al-Sady B, Quail PH, and Monte E (2016). Molecular convergence of clock and photosensory pathways through PIF3-TOC1 interaction and co-occupancy of target promoters. Proc Natl Acad Sci U S A 113, 4870–4875. [PubMed: 27071129]

Soy J, Leivar P, Gonzalez-Schain N, Sentandreu M, Prat S, Quail PH, and Monte E (2012). Phytochrome-imposed oscillations in PIF3 protein abundance regulate hypocotyl growth under diurnal light/dark conditions in Arabidopsis. Plant J 71, 390–401. [PubMed: 22409654]

Suarez-Lopez P, Wheatley K, Robson F, Onouchi H, Valverde F, and Coupland G (2001). CONSTANS mediates between the circadian clock and the control of flowering in Arabidopsis. Nature 410, 1116–1120. [PubMed: 11323677]

Thomas PD, Campbell MJ, Kejariwal A, Mi H, Karlak B, Daverman R, Diemer K, Muruganujan A, and Narechania A (2003). PANTHER: a library of protein families and subfamilies indexed by function. Genome Res 13, 2129–2141. [PubMed: 12952881]

Toledo-Ortiz G, Johansson H, Lee KP, Bou-Torrent J, Stewart K, Steel G, Rodriguez-Concepcion M, and Halliday KJ (2014). The HY5-PIF regulatory module coordinates light and temperature control of photosynthetic gene transcription. PLoS Genet 10, e1004416. [PubMed: 24922306]

Viczian A, Kircher S, Fejes E, Millar AJ, Schafer E, Kozma-Bognar L, and Nagy F (2005). Functional characterization of phytochrome interacting factor 3 for the Arabidopsis thaliana circadian clockwork. Plant Cell Physiol 46, 1591–1602. [PubMed: 16055924]

Wickham H (2009). ggplot2: Elegant Graphics for Data Analysis. Springer-Verlag New York.

Xu H, Liu Q, Yao T, and Fu X (2014). Shedding light on integrative GA signaling. Curr Opin Plant Biol 21, 89–95. [PubMed: 25061896]

Xu X, Paik I, Zhu L, and Huq E (2015). Illuminating Progress in Phytochrome-Mediated Light Signaling Pathways. Trends Plant Sci 20, 641–650. [PubMed: 26440433]

Yeom M, Kim H, Lim J, Shin AY, Hong S, Kim JI, and Nam HG (2014). How do phytochromes transmit the light quality information to the circadian clock in Arabidopsis? Mol Plant 7, 1701–1704. [PubMed: 25095795]

Zhang Y, Liu T, Meyer CA, Eeckhoute J, Johnson DS, Bernstein BE, Nusbaum C, Myers RM, Brown M, Li W, et al. (2008). Model-based analysis of ChIP-Seq (MACS). Genome Biol 9, R137. [PubMed: 18798982]

Zhang Y, Mayba O, Pfeiffer A, Shi H, Tepperman JM, Speed TP, and Quail PH (2013). A quartet of PIF bHLH factors provides a transcriptionally centered signaling hub that regulates seedling

morphogenesis through differential expression-patterning of shared target genes in Arabidopsis. PLoS Genet 9, e1003244. [PubMed: 23382695]

Zheng H, Zhang F, Wang S, Su Y, Ji X, Jiang P, Chen R, Hou S, and Ding Y (2018). MLK1 and MLK2 Coordinate RGA and CCA1 Activity to Regulate Hypocotyl Elongation in Arabidopsis thaliana. Plant Cell 30, 67–82. [PubMed: 29255112]

Zhu JY, Oh E, Wang T, and Wang ZY (2016). TOC1-PIF4 interaction mediates the circadian gating of thermoresponsive growth in Arabidopsis. Nat Commun 7, 13692. [PubMed: 27966533]

Zielinski T, Moore AM, Troup E, Halliday KJ, and Millar AJ (2014). Strengths and limitations of period estimation methods for circadian data. PLoS One 9, e96462. [PubMed: 24809473]

Highlights

- The clock component GI gates light signaling through direct regulation of PIFs
- GI modulates PIF transcriptional activity via several distinct molecular mechanisms
- Gating of PIF activity by GI is required to time key output processes such as growth rate
- Regulation of PIF activity by GI is required for optimal circadian clock progression

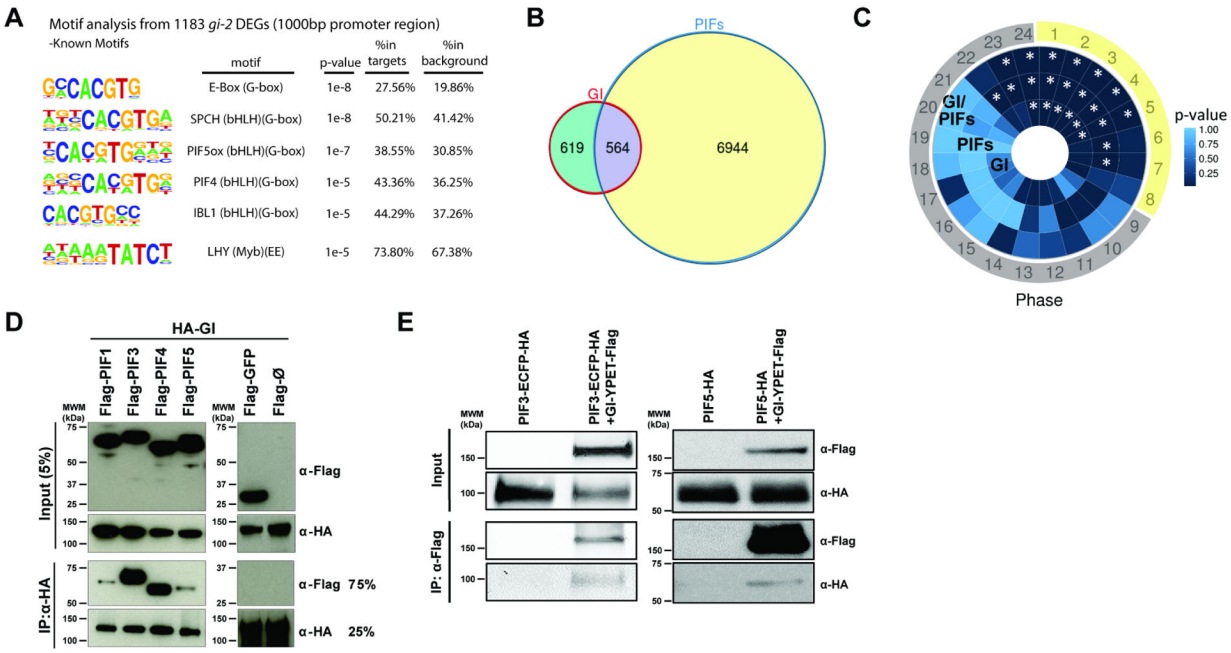

Figure 1. GI shares targets with light signaling components and interacts with PIF proteins.

(A) Over-represented *cis* motifs at the promoter regions of *gi-2* DEGs.

(B) Overlap between DEGs in *gi-2* and a comprehensive set of PIF-regulated genes (intersection p<2.2e-16).

(C) Phase enrichment heatmap depicting the p-value of the phase of peak expression enrichment (count/expected) of genes differentially expressed in *gi-2* only (GI), regulated by PIFs only (PIFs), and potentially regulated by GI and PIFs (GI-PIFs) under SD conditions (*p<0.01). Day period is marked in yellow and night period in gray.

(D) *In vitro* pull-down assays showing the interaction between GI and PIFs (PIF1, PIF3, PIF4, and PIF5).

(E) *In vivo* co-immunoprecipitations in *Arabidopsis* transgenic seedlings expressing GI-YPET-Flag and PIF3-ECFP-HA (left panel), and GI-YPET-Flag and PIF5-HA (right panel) tagged protein versions.

See also Figure S1 and Table S1.

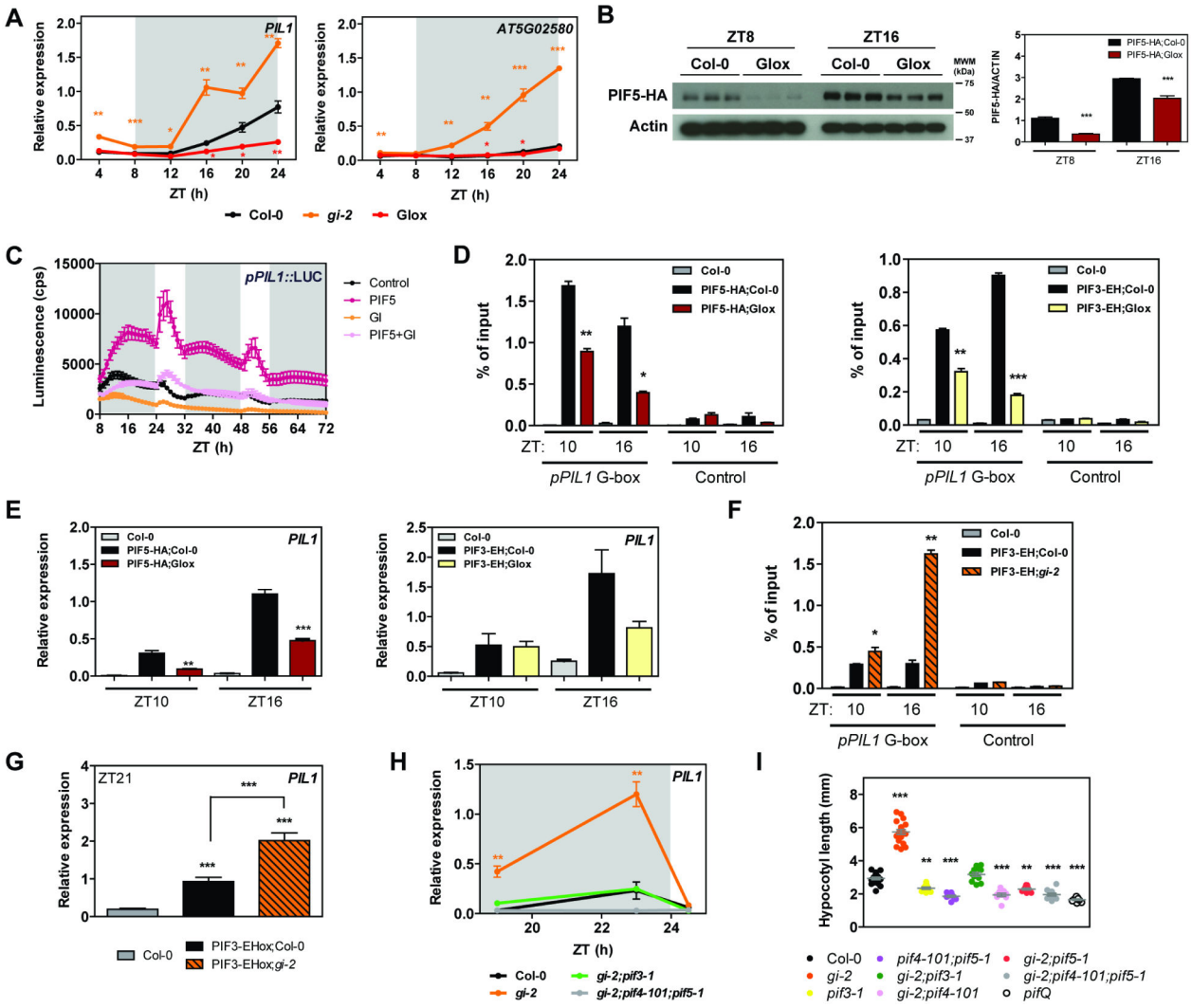

Figure 2. GI modulates PIF stability and activity.

(A) Relative expression of *PIL1* and *AT5G02580* in wildtype (Col-0), *gi-2*, and GIox seedlings grown for 10 days in SDs (mean ± SEM of 3 biological replicates). White and gray shadings represent day and night, respectively.

(B) PIF5-HA protein accumulation at ZT8 and 16 in the indicated backgrounds under SD conditions. Protein levels were normalized against ACTIN levels. The quantitation is shown on the right (mean ± SEM of 3 biological replicates).

(C) Transactivation assays in *N. benthamiana* leaves. Different effectors were co-expressed with the *pPIL1*::LUC reporter construct. Luminescence was measured 2 days post-infiltration in SD conditions. Results show mean ± SEM (n=12).

(D and F) ChIP assays of 10-day-old seedlings grown in SD conditions and harvested at the indicated ZTs. The enrichment of the specified regions in the immunoprecipitated samples was quantified by qPCR. Values represent mean ± SEM (n=2–4).

(E, G, and H) Relative expression of *PIL1* in the indicated backgrounds in SDs (mean ± SEM of 3 biological replicates). White and gray shadings represent day and night, respectively.

(I) Hypocotyl length measurements from the indicated lines grown for 14 days in SDs (in gray, mean ± SEM, n=16–22).
(A-I) *p<0.05, **p<0.01, ***p<0.001 Student's *t*-test (A-H) or Tukey's multiple comparisons test (I).
See also Figures S2 and S3.

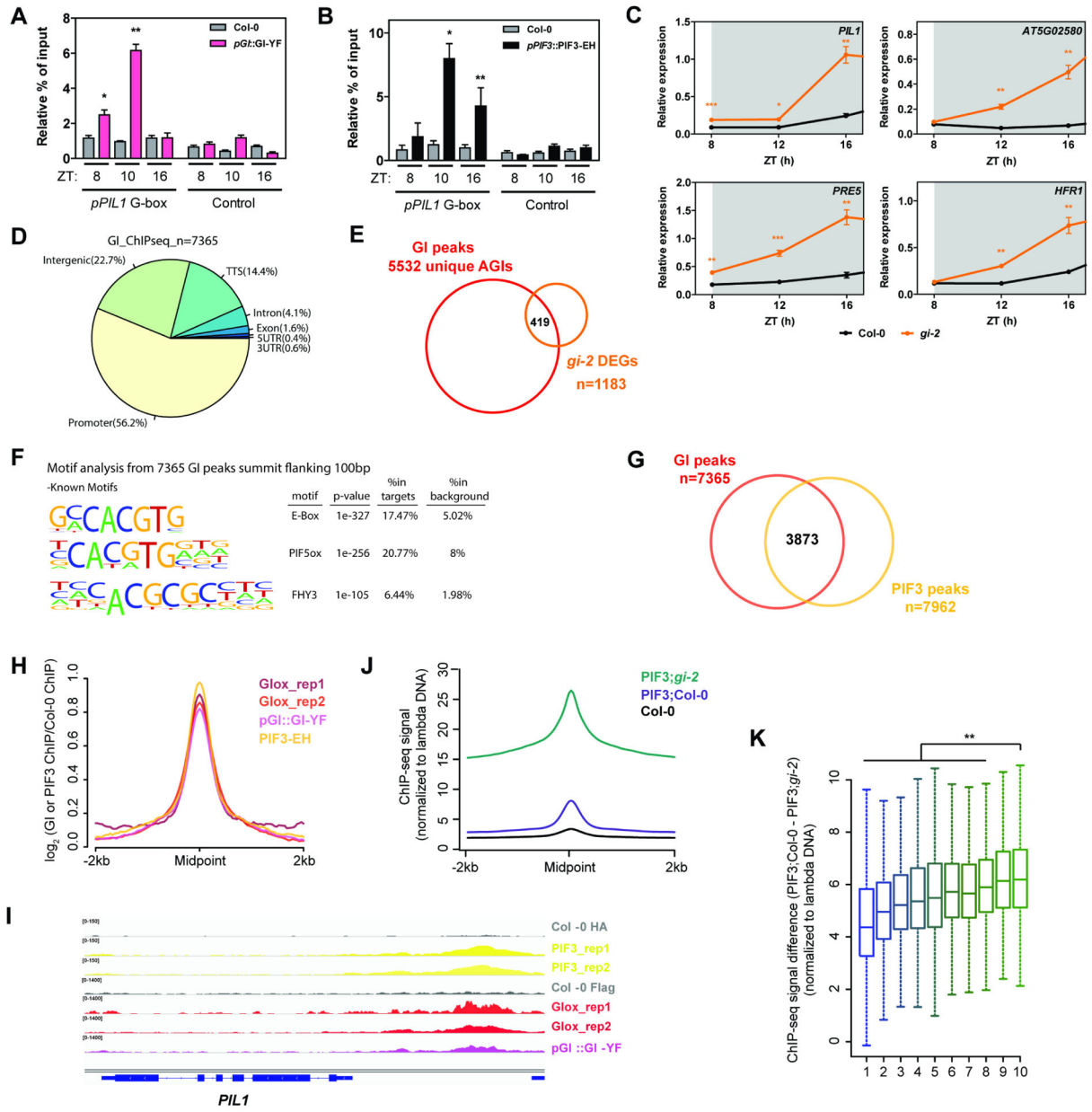

Figure 3. GI and PIFs occupy the same genomic targets in a phase dependent pattern.

(A and B) ChIP assays of 10-day-old seedlings grown in SD conditions and harvested at the indicated ZTs. The enrichment of the specified regions in the immunoprecipitated samples was quantified by qPCR. Values represent mean ± SEM of 3 independent experiments (n=2–4; *p<0.05, **p<0.01 Student's *t*-test). To account for experimental noise, the enrichment in each replicate was calculated as % of input and normalized to the enrichment of *pPIL1* fragments in Col-0.

(C) Relative expression of the indicated PIF targets in wildtype (Col-0) and *gi-2* during early night in SDs (mean ± SEM of 3 biological replicates; *p<0.05, **p<0.01, ***p<0.001 Student's *t*-test; data from Figure 2A and S2A is re-plotted). White and gray shadings represent day and night, respectively.

(D) Genomic annotation of GI ChIP-seq peaks. The midpoint of the peaks was used for this analysis.
(E) Overlap between GI ChIP-seq targets and *gi-2* DEGs.
(F) Over-represented *cis* elements around the summit of GI ChIP-seq peaks (±100 bp flanking region).
(G) Overlap between GI and PIF3 ChIP-seq peaks (hypergeometric test $p<0.01$).
(H) Metaplot of the signal from PIF3 and GI ChIP-seqs plotted over the centers of PIF3 peaks.
(I) Visualization of PIF3 and GI ChIP-seq data in the genomic region encompassing the *PIL1* locus.
(J) Quantitative analysis of the signal in PIF3-EH;Col-0 and PIF3-EH;*gi-2* ChIP-seqs plotted over the centers of PIF3 peaks (n=7962). The ChIP-seq signal in each sample was additionally normalized to a spiked in control (unmethylated lambda DNA).
(K) Boxplot of the signal difference between quantitative PIF3-EH;Col-0 and PIF3-EH;*gi-2* ChIP-seqs over GI peaks ranked by increasing signal and divided in 10 groups (deciles 1 to 10). Statistically significant differences between mean values by Welch's two sample *t*-test in each decile relative to the 10^{th} decile are shown (**$p<0.01$).
See also Figure S4 and Table S1.

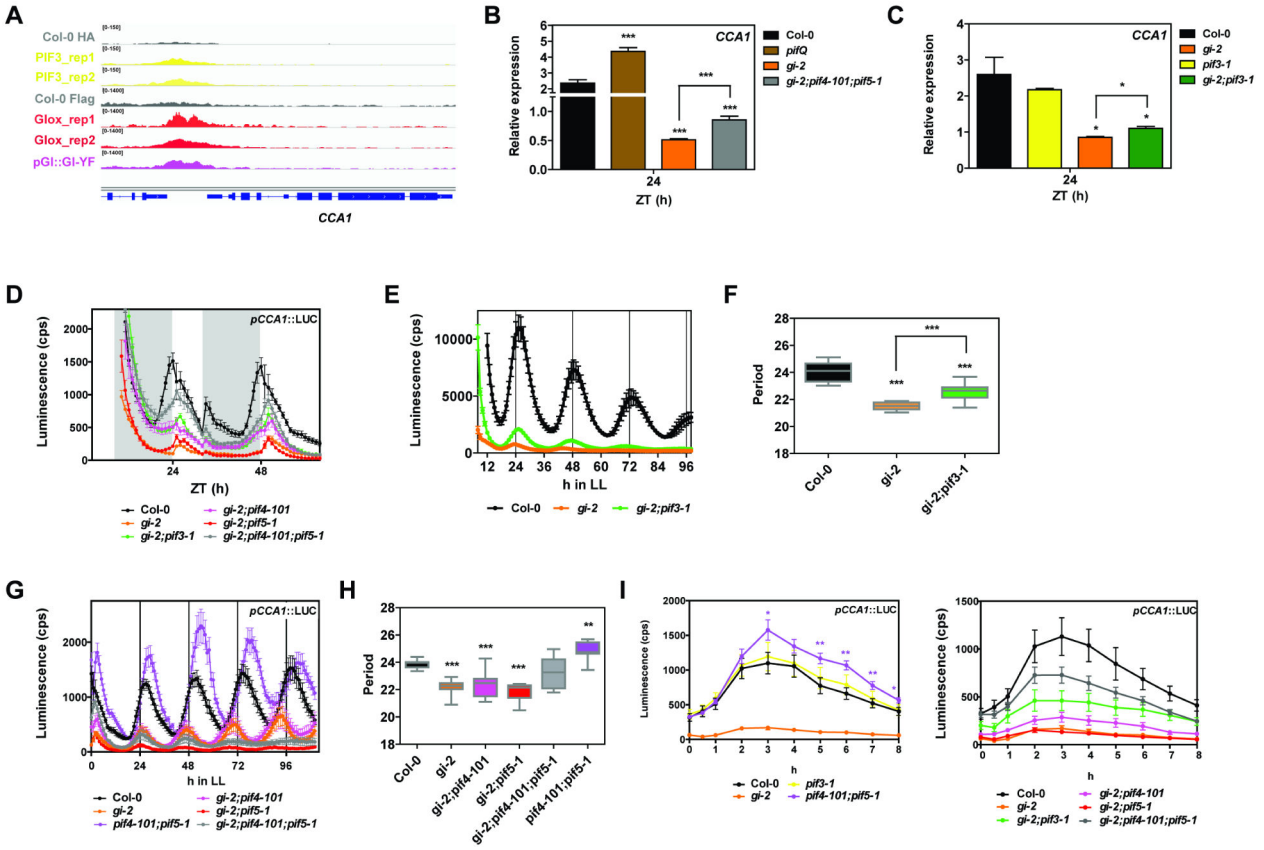

Figure 4. GI modulation of light signaling affects circadian rhythms.

(A) Visualization of PIF3 and GI ChIP-seq data in the genomic region encompassing the *CCA1* locus.

(B and C) Relative expression of *CCA1* in the indicated backgrounds at ZT24 in SDs (mean ± SEM of 3 biological replicates).

(D) Bioluminescence analysis of *pCCA1*::LUC in seedlings in SD conditions (mean ± SEM, n=12). White and gray bars represent day and night, respectively.

(E and G) Bioluminescence analysis of *pCCA1*::LUC in constant light (LL) (mean ± SEM, n=12). Plants were entrained in SDs for 7 days.

(F and H) Period length estimations of *pCCA1*::LUC reporter expression in the experiments shown in E and G as analyzed by FTT-NLLS (n=12).

(I) Bioluminescence analysis of *pCCA1*::LUC activation in 3 day old etiolated seedlings transferred to light (mean ± SEM, n=12).

(B-I) *p<0.05, **p<0.01, ***p<0.001 Student's *t*-test.

See also Figure S5.

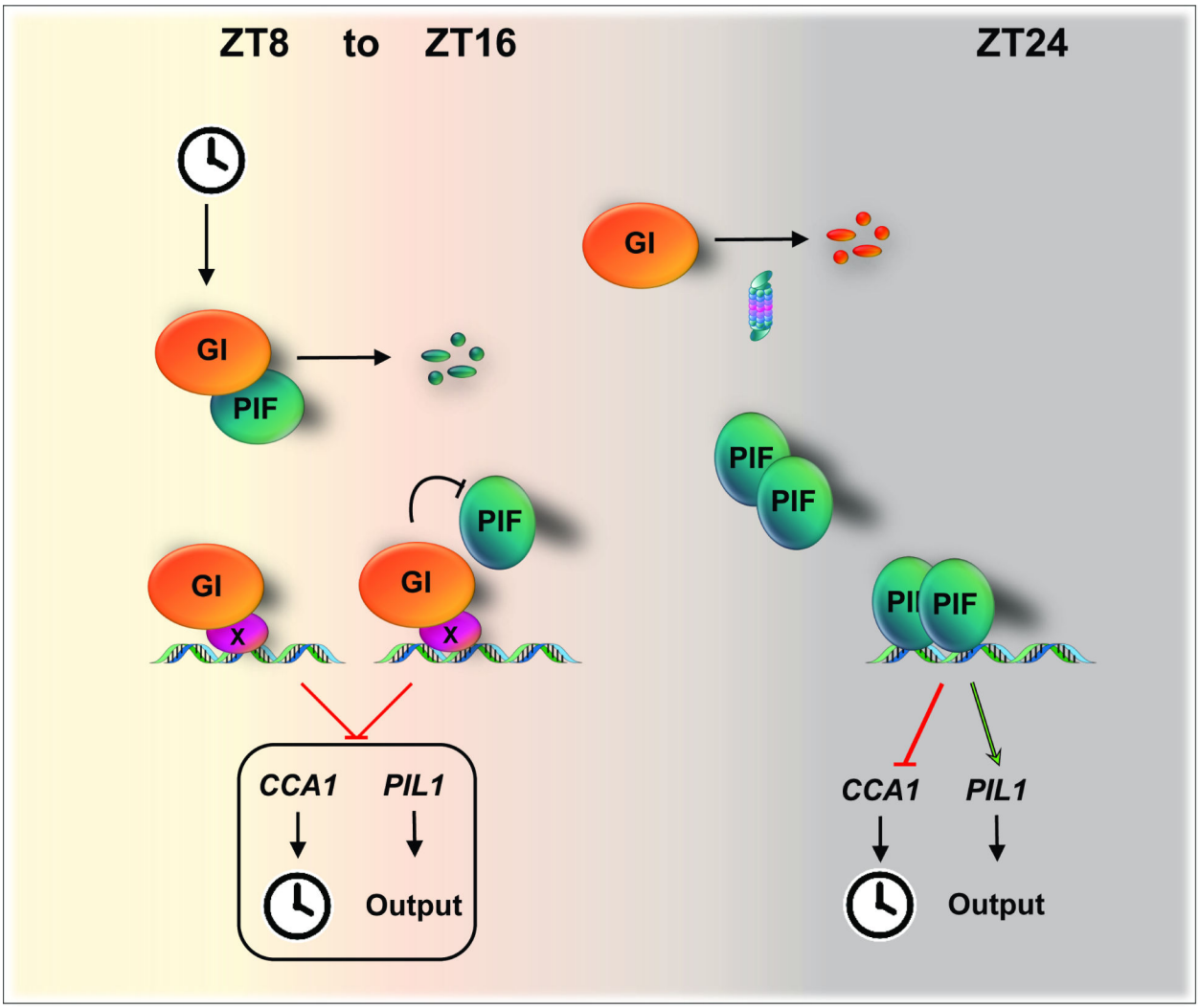

Figure 5. Model depicting the function of GI in the circadian gating of light signaling pathways.

As GI accumulates during the early night, it prevents the binding of the PIFs to chromatin through direct interaction and competition for target promoter regions. Progressive degradation of GI later at night enables the release of the PIFs, which accumulate and access target promoter regions at this time. The proposed mechanism is required not only to adequately phase output rhythms such as growth, but also to set the pace of the clock.

KEY RESOURCE TABLE

REAGENT or RESOURCE	SOURCE	IDENTIFIER
Antibodies		
Anti-FLAG M2	Sigma	Cat# F1804; RRID:AB_262044
Anti-FLAG-HRP	Sigma	Cat#A8592; RRID:AB_439702
Anti-HA 3F10	Roche	Cat# 11867423001; RRID:AB_2314622
Anti-HA-HRP	Roche	Cat# 12013819001; RRID: AB_390917
Anti-Actin	Millipore	Cat# MAB1501; RRID:AB_2223041
Anti-Mouse-HRP	BioRad	Cat#1706516
Bacterial and Virus Strains		
E. coli ccdB survival	Invitrogen	A10460
E. coli TOP10	Invitrogen	C404003
Agrobacterium tumefaciens strain GV3101	N/A	N/A
Agrobacterium tumefaciens strain C58	N/A	N/A
Chemicals, Peptides, and Recombinant Proteins		
Hygromycin B	Invitrogen	Cat# 10687010
Glufosinate ammonium (BASTA)	Sigma	Cat#45520
PMSF	Sigma	Cat# P7626
Complete EDTA-free Protease Inhibitor	Roche	Cat# 11836170001
Phosphatase Inhibitor 2	Sigma	Cat#P5726
Phosphatase Inhibitor 3	Sigma	Cat#P0044
MG-132	Peptides International	Cat#3175-v
Protein G Dynabeads	Invitrogen	Cat# 10004D
GlycoBlue	Invitrogen	Cat# AM9515
D-Luciferin, potassium salt	Biosynth AG	Cat#L-8220
Critical Commercial Assays		
Gateway BP clonase enzyme mix	Invitrogen	Cat#11789020
Gateway LR clonase enzyme mix	Invitrogen	Cat#11791100
ProQuest™ Two-Hybrid System	Invitrogen	Cat#PQ1000101
TnT® SP6 High-Yield Wheat Germ Protein Expression System	Promega	Cat#L3260
DC Protein Assay	BioRad	Cat#5000116
Supersignal West Pico, Dura, and Femto substrates	Pierce	Cat#34577, 34075, 34095
iScript cDNA synthesis kit	BioRad	Cat#1708890
Maxima SYBR Green qPCR Master Mix	Thermo Scientific	Cat#K0253
Ovation® Ultralow V2 kit	NuGEN	Cat# 0344NB-A01
Deposited Data		
ChIP-seq data	This paper	GSEXXXXX
Experimental Models: Organisms/Strains		

REAGENT or RESOURCE	SOURCE	IDENTIFIER
Col-0	N/A	N/A
gi-2	Fowler et al., 1999	N/A
GIox	David et al., 2006	N/A
PIF5-HA	Lorrain et al., 2008	N/A
PIF4-Flash	Pedmale et al., 2016	N/A
pif3-1	Kim et al., 2003	SALK_030753
pif4-101	Lorrain et al., 2008	Garlic_114_G06
pif5-1	Fujimori et al., 2004	SALK_087012
pifQ	Leivar et al., 2008	N/A
CCA1::LUC	Salome and McClung, 2005	N/A
gi-2;pif3-1	This paper	N/A
gi-2;pif4-101	This paper	N/A
gi-2;pif5-1	This paper	N/A
gi-2;pif4-101;pif5-1	This paper	N/A
GI-YPET-Flag	This paper	N/A
pGI::GI-YPET-Flag	This paper	N/A
PIF3-ECFP-HA	This paper	N/A
pPIF3::PIF3-ECFP-HA	This paper	N/A
PIF3-ECFP-HA;GI-YPET-Flag	This paper	N/A
PIF3-ECFP-HA;*gi-2*	This paper	N/A
pGI::GI-YPET-Flag;pPIF3::PIF3-ECFP-HA	This paper	N/A
PIF5-HA;GI-YPET-Flag	This paper	N/A
pCCA1::LUC, *gi-2;pif3-1*	This paper	N/A
pCCA1::LUC; *gi-2;pif4-101*	This paper	N/A
pCCA1::LUC; *gi-2;pif5-1*	This paper	N/A
pCCA1::LUC; *gi-2;pif4-101;pif5-1*	This paper	N/A
pCCA1::LUC; PIF3-ECFP-HA	This paper	N/A
pCCA1::LUC; PIF5-HA	This paper	N/A
pCCA1::LUC; PIF4-Flash	This paper	N/A
Oligonucleotides		
Primers used in this study, see Table S2		
Recombinant DNA		
pD32-GI	This paper	N/A
pD22-PIF1	Pruneda-Paz et al., 2014	N/A
pD22-PIF3	Pruneda-Paz et al., 2014	N/A
pD22-PIF4	Pruneda-Paz et al., 2014	N/A
pD22-PIF5	Pruneda-Paz et al., 2014	N/A
pTNT-HA	Chory lab	N/A
pTNT-Flag	Chory lab	N/A

REAGENT or RESOURCE	SOURCE	IDENTIFIER
pTNT-HA-GI	This paper	N/A
pTNT-Flag-PIF1	This paper	N/A
pTNT-Flag-PIF3	This paper	N/A
pTNT-Flag-PIF4	This paper	N/A
pTNT-Flag-PIF5	This paper	N/A
pTNT-Flag-GFP	This paper	N/A
pTNT-Flag-P3-1	This paper	N/A
pTNT-Flag-P3-2	This paper	N/A
pTNT-Flag-P3-3	This paper	N/A
pTNT-Flag-P3-4	This paper	N/A
pB7m34GW	University of Ghent collection	https://gateway.psb.ugent.be
pB-35S::GI-YPET-Flag	This paper	N/A
pB-pGI::GI-YPET-Flag	This paper	N/A
pH7m34GW	University of Ghent collection	https://gateway.psb.ugent.be
pH-35S::PIF3-ECFP-HA	This paper	N/A
pH-pPIF3::PIF3-ECFP-HA	This paper	N/A
pEarleyGate201	Earley et al., 2006	N/A
pEarleyGate202	Earley et al., 2006	N/A
pEG201-PIF3	This paper	N/A
pEG201-PIF5	This paper	N/A
pEG201-GFP	This paper	N/A
pEG202-PIF1	This paper	N/A
pEG202-PIF3	This paper	N/A
pEG202-PIF4	This paper	N/A
pEG202-PIF5	This paper	N/A
pEG201-GI	This paper	N/A
pEG201-GFP	This paper	N/A
pGreenII 0800-LUC	Hellens et al., 2005	N/A
pGLUCpPIL1	This paper	N/A
pGLUCpCCA1	This paper	N/A
Software and Algorithms		
VisionWorksLS	UVP, LLC	N/A
NIH ImageJ software	Schneider et al., 2012	https://imagej.nih.gov/ij/
CFX Manager	BioRad	Cat#1845000
LabView	National Instruments	N/A
BioDare2	Moore et al., 2014; Zielinski et al., 2014	https://www.biodare2.ed.ac.uk
Bowtie (v1.0.0)	Langmead et al., 2009	http://bowtie-bio.sourceforge.net/index.shtml
MACS2 (v 2.1.1.)	Zhang et al., 2008	https://pypi.org/project/MACS2/
NGSplot (v 2.41.4)	Shen et al., 2014	https://github.com/shenlab-sinai/ngsplot

REAGENT or RESOURCE	SOURCE	IDENTIFIER
HOMER	Heinz et al., 2010	http://homer.ucsd.edu/homer/download.html
Phaser	Mockler et al., 2007	http://phaser.mocklerlab.org/
PANTHER	Thomas et al., 2003	http://www.pantherdb.org/
R	RCoreTeam, 2016	http://www.R-project.org/
ggplot2 plotting package	Wickham, 2009	https://cran.r-project.org/web/packages/ggplot2/